HOW BLACKBERRY SHAPES MITOCHONDRIAL FUNCTION IN OBESITY?

MARIA INÊS ROCHA MOREIRA TEIXEIRA DUARTE

A dissertation submitted in partial fulfillment of the requirements for the Degree of Masters in Biomedical Research (Specialization Area: Ageing and Chronic Diseases) at Faculdade de Ciências Médicas | NOVA Medical School of NOVA University Lisbon

September, 2025

nms.unl.pt

HOW BLACKBERRY SHAPES MITOCHONDRIAL FUNCTION IN OBESITY?

Maria Inês Rocha Moreira Teixeira Duarte
Supervisor: Ana Faria, Associate Professor at NOVA Medical School

A dissertation submitted in partial fulfillment of the requirements for the Degree of Masters in Biomedical Research (Specialization Area: Ageing and Chronic Diseases)

September, 2025

Aknowledgements

This dissertation is the result of the unwavering support I have received over the past two years from many people. Without them, this work would not have been possible.

First and foremost, I would like to express my deepest gratitude to Professor Ana. From the very beginning, she allowed me to shape a project tailored to my own interests, always made herself available whenever I needed, and guided me through every single step. She ensured that I was never alone and that I was constantly learning throughout the process. Professor Ana embodies what a true supervisor and teacher should be, and I feel privileged to have had the opportunity to work so closely and learn under her guidance.

I am also deeply grateful to Professor João Araújo, who, in the last months of my work, became an essential part of my learning and supervision. With him, beyond learning Western Blot inside out, I came to understand, most importantly, why lab work should never be done alone.

To all the members of the Metabolism and Nutrition Lab at NOVA Medical School, thank you for creating, since day one, such a welcoming environment where everyone immediately feels part of the group. In particular, I would like to sincerely thank Maria João Almeida, Shámila Ismael, Catarina Rodrigues, and Gilberto Maia Santos. Each of you supported me in valuable ways: from teaching me methods, covering for me when I could not be present, or even simply sending me relevant information for my project. These small but important gestures made my work possible, and I am truly grateful for the support and team spirit that you brought into this journey.

To my family, the biggest thank you of all. To my mom, whose warm hugs and constant encouragement remind me that family always comes first, and that with the support of our loved ones we can achieve what we set out to do. To my father, who not only taught me the importance of critical thinking but always reassure me that, as long as I keep learning, everything is fine. To Vasco, my person, who is always there for me, who lifts me up when I fall and celebrates my successes as if they were his own. And to my grandparents, who, between their quiet presence and the loud noise of the television, create the home where I feel safest.

This work is the product of two very busy years, but also two of the most enriching years of my life. This thesis may bear my name, but it stands as proof that no work is ever accomplished alone: it is only possible thanks to the network of support that stands behind it.

Campo Mártires da Pátria, 130
1169-056 Lisboa · Portugal

Abstract

Background:

Obesity is closely associated with mitochondrial dysfunction in adipose tissue, leading to impaired metabolism and increased risk of chronic disease. Blackberries (BB) are rich in anthocyanins, particularly cyanidin-3-glucoside (C3G), which is metabolized by the gut microbiota into protocatechuic acid (PCA) and promotes the growth of bacteria that produce indole-3-propionic acid (IPA). C3G, PCA, and IPA are all believed to influence mitochondrial function.

Objective:

The objective of this study was to investigate the effects of BB, C3G, and associated compounds, PCA and IPA, on mitochondrial features and dynamics in the context of obesity.

Material and Methods:

Two models were used: an *in vivo* model of mice with obesity induced by high-fat diet and fecal microbiota transplantation and an *in vitro* model of insulin-resistant (IR) 3T3-L1 adipocytes. In mice, visceral white adipose tissue was analyzed for mitochondrial content and for the expression of metabolic and thermogenic markers. In adipocytes, cells were treated with BB and its related compounds and evaluated for their effects on mitochondrial content, ATP levels, ROS production, and the expression of genes and proteins relevant to mitochondrial activity, including those involved in fusion, fission, and biogenesis.

Results:

BB supplementation in mice increased mtDNA copy number. In 3T3-L1 adipocytes, IR elevated ATP levels, while all treatments reduced them, consistent with changes in mitochondrial coupling. IPA restored mtDNA levels under IR, whereas C3G reduced them. PCA restored both fusion (MFN2) and fission (DRP1) markers, while PCA and C3G influenced biogenesis. UCP1 expression increased with IR but was reduced by BB and PCA, and PGC1α expression was differentially modulated by treatments.

Conclusion:

BB and its related compounds may be involved in the modulation of mitochondrial adaptations in obesity, with distinct compound-specific effects. These findings suggest their potential as interventions to target mitochondrial dysfunction in metabolic diseases, highlighting the importance of whole-fruit consumption and the role of the host metabolism.

Keywords:

Adipocytes, adipose tissue, blackberry, cyanidin-3-glucoside, indole-3-propionic acid, mitochondria, obesity, protocatechuic acid.

Campo Mártires da Pátria, 130
1169-056 Lisboa · Portugal

Resumo

Introdução:

A obesidade está associada à disfunção mitocondrial no tecido adiposo, conduzindo a alterações metabólicas e a um risco acrescido de doenças crónicas. As amoras (BB) são ricas em antocianinas, nomeadamente cianidina-3-glicosídeo (C3G), que é metabolizada pelo microbiota intestinal em ácido protocatecuico (PCA) e promove o crescimento de bactérias produtoras de ácido indol-3-propiônico (IPA). Considera-se que a C3G, o PCA e o IPA influenciem a função mitocondrial.

Objetivo:

O objetivo deste estudo era investigar os efeitos da BB, da C3G e dos compostos associados, PCA e IPA, nas características e dinâmica mitocondrial em contexto de obesidade.

Metodologia:

Foram utilizados dois modelos: um modelo *in vivo* de ratinhos com obesidade induzida por dieta rica em gordura e por transplante de microbiota fecal, e um modelo *in vitro* de adipócitos 3T3-L1 resistentes à insulina (IR). Nos ratinhos, o tecido adiposo branco visceral foi analisado quanto ao conteúdo mitocondrial e à expressão de marcadores metabólicos e termogénicos. Nos adipócitos, as células foram tratadas com BB e os seus compostos associados e avaliadas quanto ao conteúdo mitocondrial, níveis de ATP, produção de espécies reativas de oxigénio (ROS) e expressão de genes e proteínas relevantes para a atividade mitocondrial, incluindo os envolvidos em processos de fusão, fissão e biogénese.

Resultados:

A suplementação com BB em ratinhos aumentou o número de cópias de mtDNA. Nos adipócitos 3T3-L1, a resistência à insulina aumentou os níveis de ATP, enquanto todos os tratamentos os reduziram, concordante com alterações no acoplamento mitocondrial. O IPA restaurou os níveis de mtDNA sob IR, enquanto a C3G os reduziu. O PCA restaurou os marcadores de fusão (MFN2) e de fissão (DRP1), enquanto o PCA e a C3G influenciaram a biogénese. A expressão de UCP1 aumentou em condições de IR, mas foi reduzida pela BB e pelo PCA. A expressão de PGC1α foi diferencialmente modulada pelos diferentes tratamentos.

Conclusão:

A BB e os seus compostos associados podem estar envolvidos na modulação das adaptações mitocondriais em contexto de obesidade, apresentando efeitos distintos e específicos. Estes resultados sugerem o seu potencial em intervenções no combate à disfunção mitocondrial em doenças metabólicas, destacando a relevância do consumo da fruta inteira e o papel de cada metabolismo em causa.

Palavras-chave:

Ácido indol-3-propiônico, ácido protocatecuico, adipócitos, amora, cianidina-3-glicosídeo, mitocôndria, obesidade, tecido adiposo.

Campo Mártires da Pátria, 130
1169-056 Lisboa · Portugal

Table of Contents

Campo Mártires da Pátria, 130
1169-056 Lisboa · Portugal

Campo Mártires da Pátria, 130
1169-056 Lisboa · Portugal

List of Figures

Campo Mártires da Pátria, 130
1169-056 Lisboa · Portugal

Campo Mártires da Pátria, 130
1169-056 Lisboa · Portugal

List of Tables

Campo Mártires da Pátria, 130
1169-056 Lisboa · Portugal

Abbreviations

AT	Adipose Tissue
ATP	Adenosine Triphosphate
BB	Blackberry
C3G	Cyanidin-3-O-Glucoside
CO_2	Carbon Dioxide
DCF	2',7'-Dichlorofluorescein
DCFH	2',7'-Dichlorodihydrofluorescein
DCFH-DA	2',7'-Dichlorodihydrofluorescein Diacetate
DGAV	Portuguese Directorate-General for Food and Veterinary Affairs
DIM	Differentiation Induction Medium
DMEM	Dulbecco's Modified Eagle's Medium
DPM	Differentiation Progression Medium
DRP1	Dynamin-Related Protein 1
DXM	Dexamethasone
FBS	Fetal Bovine Serum
FGF21	Fibroblast Growth Factor 21
FMT	Fecal Microbiota Transplantation
IBMX	3-Isobutyl-1-Methylxanthine
IPA	Indole-3-Propionic Acid
IR	Insulin Resistance
MFN1/MFN2	Mitofusin 1/Mitofusin 2
MONET	Unravelling Microbiota-Gut-Brain Axis Pathways in Obesity-Associated Neuroinflammation: The Blackberry Signature Study
mtDNA	mitochondrial DNA
NCDs	Non-communicable diseases
nDNA	nuclear DNA
OXPHOS	Oxidative Phosphorylation
PBS	Phosphate-Buffered Saline
PCA	Protocatechuic Acid
P-S	Penicillin–Streptomycin
qPCR	Quantitative real-time PCR
ROS	Reactive Oxygen Species
SEM	Standard Error of the Mean
TPBS	PBS containing 0.1% Tween-20
WAT	White Adipose Tissue
WHO	World Health Organization

Campo Mártires da Pátria, 130
1169-056 Lisboa · Portugal

Introduction

Obesity: A Global Health Challenge

Obesity is a chronic and multifactorial disease, characterized by increased adipose tissue (AT) mass and significant repercussions across different organs and systems, that significantly contributes to the global burden of non-communicable diseases (NCDs) (1, 2).

According to the World Health Organization (WHO), in 2022 2.5 billion adults (≥18 years) were overweight, and among them, 890 million were living with obesity (3).Based on the latest estimates by the NCD Risk Factor Collaboration, if no significant interventions are implemented to alter current trends, the global prevalence of overweight and obesity will continue to rise. In fact, it is projected that by 2030, 50% of adult men and women will be living with overweight, and 17% of men and 22% of women will be living with obesity (1).

Considering the global challenges that this disease imposes, it is essential that all sectors of society collaborate to develop solutions to address effectively this issue and create sustainable systems that would endure over time.

Even though the research in obesity has been increasing in the last years, there are still many gaps to understand this disease. In fact, in 2025, The Lancet Diabetes & Endocrinology Commission published a new work on the definition and diagnostic criteria of clinical obesity, suggesting that a clear consensus on the disease is still evolving. This reflects the ongoing need for studies that can deepen our understanding of obesity and support the development of more effective treatment strategies (4).

The Adipose Tissue and the Mechanisms Underlying Obesity

Obesity arises from a complex interplay of environmental, genetic, and physiological factors. In modern societies, environments increasingly promote behaviours that favour energy imbalance (such as high-calorie food consumption, sedentary lifestyles, and disrupted sleep patterns), which create conditions that do not promote the maintenance of a healthy body weight. However, individual susceptibility to these obesogenic conditions varies, in part due to genetic and metabolic differences. The latter ones are tightly connected to the function of AT, a central organ in energy storage and homeostasis (5).

AT is a specialized connective tissue that contains adipocytes and several other cell types, embedded within capillary and innervation networks that function together as an integrated unit. Although lipid storage, thermal activity, and mechanical insulation are well recognized classical functions of AT, it is also considered a multifunctional, metabolically highly active, immune, and endocrine organ that directly modulates many processes, including energy balance and metabolism. Different types of adipocytes exist: white adipocytes are specialized in energy storage, brown and beige (brite) adipocytes contribute to thermogenesis, and pink adipocytes, which appear during pregnancy, are involved in milk production (2).

In obesity, white adipose tissue (WAT) expands to store excess energy, leading to metabolic and physiological alterations. As adipocytes enlarge, they undergo functional changes, including altered signalling to the brain and peripheral organs, increased secretion of proinflammatory cytokines that contribute to insulin resistance (IR), and other metabolic changes. Organelles within AT, particularly mitochondria, play a central role in these processes (5).

Mitochondrial Dysfunction in Obesity

Mitochondria are small intracellular organelles often referred to as the "powerhouse of the cell" due to their central role in producing adenosine triphosphate (ATP), the cell's main energy source. They are also an important source of reactive oxygen species (ROS) at physiological levels. Mitochondrial dysfunction has been widely recognized as a common feature of several NCDs, including obesity, type 2 diabetes, hypertension, and dyslipidaemia (6).

Obesity is associated with changes in AT, especially WAT. White adipocytes store energy in large lipid droplets and have relatively low mitochondrial density compared to other cell types. This feature has resulted in them being relatively under-studied, despite their key role in energy storage (7). However,

Campo Mártires da Pátria, 130
1169-056 Lisboa · Portugal

it has been described that mitochondrial copy number is significantly reduced in obesity, which is linked to lower ATP production (8), and reduced expression of essential mitochondrial proteins (9).

The number and size of mitochondria are regulated by a dynamic balance between two opposing processes: fusion (joining of mitochondria to share contents and maintain function) and fission (division of mitochondria to allow turnover and quality control) (10, 11). Mitochondria are dynamic organelles that continuously undergo these processes, both in dividing and non-dividing cells, highlighting their role in maintaining cellular energy balance and homeostasis. In obesity, the balance between mitochondrial fission and fusion is often disrupted, with tissue-specific effects. In AT, reduced expression of the fission dynamin-related protein 1 (DRP1) impairs mitochondrial division, β-oxidation, and lipid metabolism. In contrast, deletion of DRP1 triggers endoplasmic reticulum stress and raises fibroblast growth factor 21 (FGF21), increasing energy expenditure and protecting against diet-induced obesity. For fusion, lower levels of mitofusin 1 and 2 (MFN1 and MFN2) in AT and hypothalamic neurons disrupt mitochondrial networks, impair energy metabolism, and increase obesity risk (12).

Beyond dynamics, mitochondrial function also depends on the expression levels of oxidative phosphorylation (OXPHOS) enzymes, which are often decreased in obesity, leading to impaired fatty acid oxidation and lower ATP production. At the same time, excessive nutrient and lipid influx in adipocytes can increase the substrate load on mitochondria, increasing the electron transport chain activity in the remaining OXPHOS complexes and promoting electron leakage, which elevates ROS production. Because mitochondrial DNA (mtDNA) lacks the repair mechanisms present in nuclear DNA (nDNA), it is particularly vulnerable to oxidative damage, and accumulated mutations can further impair OXPHOS function. Mitochondria-derived ROS also act as signaling molecules within WAT, with their effects influenced by nutritional status, hormones, and oxygen availability. Chronic oxidative stress contributes to adipocyte dysfunction by impairing insulin signaling and promoting inflammation, which further compromises mitochondrial function in AT (8).

Figure 1 summarizes the mitochondrial alterations in WAT in the context of obesity.

Given these alterations, it is important to explore strategies to counteract mitochondrial dysfunction in obesity, including the identification of compounds with properties that can directly affect it positively and could be developed as preventive or therapeutic agents.

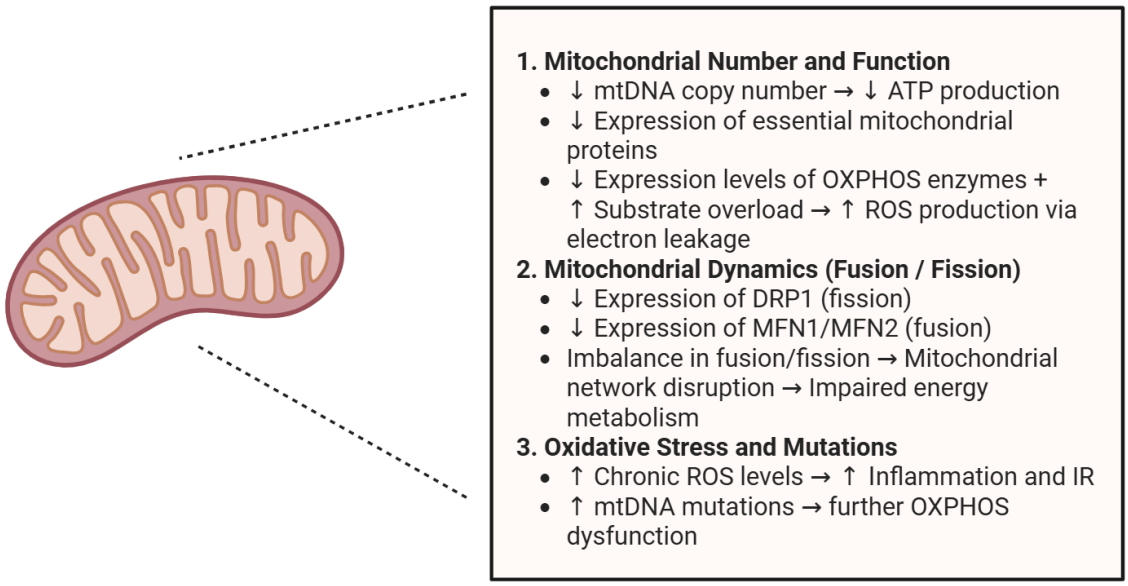

Figure 1. Summary of the mitochondrial alterations observed in white adipose tissue (WAT) in the context of obesity. Image created with BioRender.com.

Campo Mártires da Pátria, 130
1169-056 Lisboa · Portugal

Blackberry, its anthocyanins, and related metabolites

Anthocyanins are water-soluble pigments that belong to the flavonoid subgroup, responsible for the reddish-orange to bluish-purple colour of many fruits and vegetables (13, 14). Recent epidemiological studies have shown that anthocyanins exhibit antioxidant, anti-inflammatory, and anti-atherosclerotic effects and may reduce the risk of obesity-related chronic co-morbidities (15). Among these, cyanidin-3-O-glucoside (C3G) is one of the most abundant anthocyanins in nature and is particularly prevalent in blackberries, accounting for 80% of total anthocyanins in different cultivars (16, 17). This makes C3G a highly relevant target for research.

Figure 2 shows a simplified representation of the metabolic pathway of C3G following blackberry (BB) ingestion, as described below.

C3G undergoes extensive metabolism in the gastrointestinal tract, generating a variety of metabolites that can have bioactive effects. Some of these metabolites are produced directly from C3G, such as protocatechuic acid (PCA), while others arise indirectly through the modulation of the gut microbiota, such as indole-3-propionic acid (IPA).

More precisely, after ingestion, C3G begins to be metabolized in the oral cavity, where mastication, saliva, and enzymatic activity facilitate its release from the BB food matrix and initiate its degradation (18).

In the stomach, C3G is relatively stable due to the acidic conditions and can be absorbed by gastric epithelial cells (1%–10% intact, 10%–20% as first-pass metabolites). Absorption occurs mainly via active transporters, including bilitranslocase, SGLT1, GLUT1/3, and MCT1 (18).

In the small intestine, conditions are less favorable: the alkaline pH destabilizes C3G, leading to its conversion into other structures, including colorless forms (19). Factors such as brush border enzymatic activity, the ability of C3G to be released from the food matrix, and other transport mechanisms reduce its bioavailability by 40–50% in the small intestine. However, a portion of C3G is taken up into enterocytes via glucose transporters, primarily SGLT1 and GLUT2. Once inside the enterocyte, C3G can be hydrolyzed to its aglycone, cyanidin, and further metabolized through phase I (originating, for example, PCA) and phase II reactions (methylation, glucuronidation, sulfation) (18).

Despite the above, up to 85% of anthocyanins may reach the distal intestine, indicating incomplete uptake in the upper gastrointestinal tract (19). The main catabolism of C3G occurs in the distal small intestine (ileum) and upper large intestine (colon), where the gut microbiota plays a central role. Compounds that escape absorption in the small intestine reach the large intestine, where microbial enzymes perform deglucosylation to remove the glycosidic residue and cleave the C-ring, producing phenolic compounds through dehydroxylation or decarboxylation, such as PCA, which can then be absorbed or excreted. (18).

Besides C3G metabolism, several studies have reported that its intake is associated with an increase in beneficial gut bacteria, such as *Bifidobacteria*, *Lactobacillus*, and *Actinobacillus*. C3G contains a β-glucosidic bond linking it to a glucose moiety, which can be cleaved by β-glucosidase enzymes produced by these bacteria. This enzymatic breakdown provides additional energy that supports bacterial growth. Moreover, cleavage of the β-glucosidic bond releases the anthocyanidin backbone, which is further metabolized into phenolic acids, such as PCA. These metabolites contribute to lowering the intestinal pH, creating an acidic environment that further promotes the proliferation of probiotic species (20).

Moreover, it appears that manipulation of gut microbiota by anthocyanins can influence the metabolism of compounds such as tryptophan. In a study by Marques et al. (2018), rats fed a high-fat diet and supplemented with a BB anthocyanin extract showed significant changes in their intestinal microbiota composition. These microbial changes affected tryptophan metabolism, a precursor of serotonin and the kynurenine pathway. Specifically, fecal tryptophan levels were reduced in the BB-supplemented animals, suggesting an increased conversion of this amino acid into kynurenine pathway metabolites. Furthermore, urinary levels of quinurenic acid, an end product of the kynurenine pathway, were elevated in the high-fat diet rats supplemented with BB extract, indicating activation of this metabolic pathway. Although IPA was not directly measured, these microbiota alterations suggest that anthocyanin intake could potentially influence IPA production through microbial tryptophan metabolism (21). Given that IPA is a microbial metabolite derived from

Campo Mártires da Pátria, 130
1169-056 Lisboa · Portugal

tryptophan, it is plausible that microbiota shifts modulating tryptophan metabolism could also influence IPA formation, similar to their effect on kynurenine pathway metabolites.

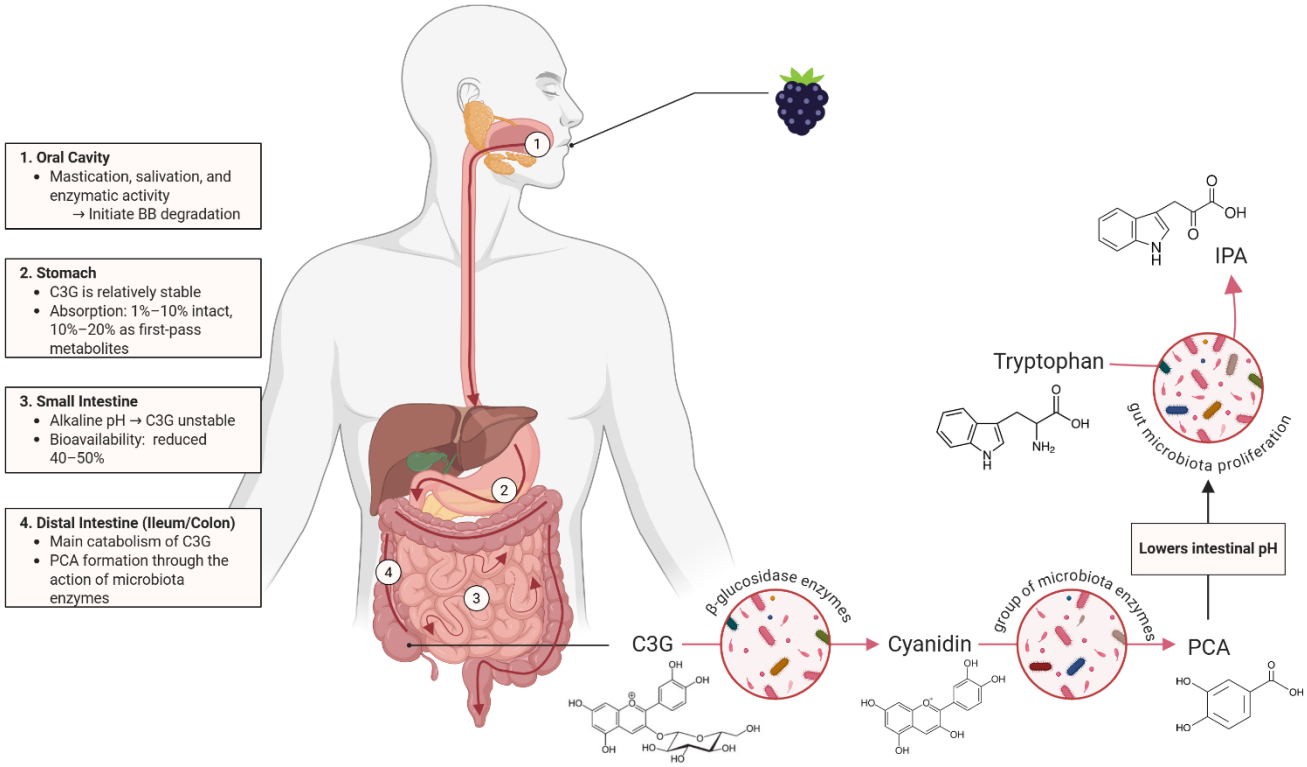

Figure 2. Catabolic process of cyanidin-3-glucoside (C3G) in the body, from ingestion in a blackberry (BB), and its main changes along the gastrointestinal tract (oral cavity, stomach, small intestine, large intestine), highlighting the production of PCA and IPA from C3G and tryptophan, and the role of gut microbiota (19, 22). Image created with BioRender.com.

Blackberry role in Obesity-Related Mitochondrial Dysfunction

BB and their components, such as anthocyanins and fiber, have been increasingly investigated as potential dietary interventions to counteract obesity-associated metabolic and mitochondrial dysfunction. Clinical studies have begun to address these effects in humans. A recent intervention in overweight and obese adults compared the impact of different berry components (anthocyanins *vs* fiber) on cellular bioenergetics. Using high-resolution respirometry of peripheral blood mononuclear cells, the study revealed that anthocyanins and fiber exerted differential effects on oxygen consumption, depending on the metabolic state. These findings highlight that distinct constituents of berries may differentially modulate mitochondrial function in humans (23).

Pre-clinical studies provide further mechanistic insight into how anthocyanins modulate the gut microbiota. In a mouse model of high-fat diet-induced metabolic syndrome, consumption of anthocyanins improved disease features, including inflammation, IR, hyperlipidaemia, and others, by altering the composition of the gut microbiota and the metabolome. Specifically, using 16S rRNA sequencing, short-chain fatty acid analysis, and fecal microbiota transplants, the study suggested that *Prevotella histicola* and acetic acid may be key players in these effects. While these findings show a clear link between anthocyanins, the microbiota, and improved metabolic health, the exact mechanisms are still not fully understood (24).

Cellular studies have also looked at how anthocyanins directly affect mitochondria. In 3T3-L1 adipocytes, treatment with C3G or BB extract showed dose-dependent effects. High-dose C3G and intermediate-dose BB extract lowered mitochondrial content but at the same time increased fatty acid–based cellular respiration. This suggests that anthocyanins may increase mitochondria efficiency in adipocytes, supporting their potential anti-obesity effects (25).

Campo Mártires da Pátria, 130
1169-056 Lisboa · Portugal

Despite growing evidence from clinical, pre-clinical, and cellular studies, important knowledge gaps remain. Many bioactive molecules, including polyphenols such as anthocyanins, have been implicated in the prevention or treatment of obesity, neurodegenerative diseases and other NCDs. However, further research is needed to delineate the precise molecular pathways underlying mitochondrial dysfunction in obesity and to unravel the mechanisms by which anthocyanins exert their beneficial effects (26). Addressing these gaps will be essential for developing novel nutritional and pharmacological approaches targeting mitochondrial dysfunction in obesity and related disorders.

Campo Mártires da Pátria, 130
1169-056 Lisboa · Portugal

Aims

The main aim of this study is to investigate the effects of BB, C3G, and the associated metabolites PCA and IPA on mitochondrial features and dynamics in AT in the context of obesity.

The specific aims of this study are:

1. Evaluate the impact of BB supplementation on mitochondrial content and gene expression of key metabolic and thermogenic markers in visceral WAT from a mice model of obesity.
2. Assess the effect of a BB extract, C3G, PCA and IPA on mitochondrial content, ATP production, ROS levels and mitochondrial dynamics in insulin-resistant 3T3-L1 adipocytes.

Campo Mártires da Pátria, 130
1169-056 Lisboa · Portugal

Materials and Methods

Visceral White Adipose Tissue from Mice

Visceral WAT from mice was obtained through a previously conducted study, as part of a pre-clinical trial named "MONET – Unravelling Microbiota-Gut-Brain Axis Pathways in Obesity-Associated Neuroinflammation: The Blackberry Signature Study." The experimental protocol is described below and represented in Figure 3. It was approved by the Portuguese Directorate-General for Food and Veterinary Affairs, DGAV (*Direção-Geral de Alimentação e Veterinária*, approval nº 0421/000/000/202) and by the Animal Welfare Responsible Organ of NOVA Medical School - NOVA University of Lisbon, NMS – UNL (approval nº 22_01_ORBEA). The fecal sample collection from human donors with obesity for mice transplant was approved by the Ethical Committee of NMS – UNL (approval no. 114/2021/CEFCM) (Supplemental Materials – Appendix 1, Appendix 2, and Appendix 3).

Male C57BL/GJ Mice

Seventy-two male C57BL/6J specific pathogen-free mice (*Mus musculus*) were obtained with 4 weeks of age and with an average weight of ±20 grams from Charles River® (Spain). All animals were housed in the NMS Bioterium and kept under controlled temperature conditions (22–24 °C), with 12 h/12 h light/dark cycles, and had *ad libitum* access to standard diet and water for 1 to 2 weeks as part of their acclimatization period before the start of the protocol.

After that, the animals were divided into 2 groups (FMT and FMT+BB), with 36 animals each. All animals had access to the same high-fat, high-sucrose diet, and underwent fecal microbiota transplantation (FMT) to induce an obese phenotype.

Fecal Microbiota

To perform fecal microbiota transplant, all mice underwent treatment with an antibiotic cocktail (ampicillin [10 mg/mL], neomycin [10 mg/mL], metronidazole [8 mg/mL], and vancomycin [5 mg/mL]) via orogastric gavage for 7 consecutive days (Day 1–7), with the aim of depleting the animals' intestinal microbiota. On the 8th day, fecal material (1 mg/mL in phosphate-buffered saline (PBS)) from 12 human donors with obesity began to be transplanted by orogastric gavage into all mice, once every 2 days over the course of a week (Day 8–14), for a total of 4 transplantations per mice.

Dietary Intervention and Supplementation

Throughout the acclimatization period until Day 14, mice were fed with a standard diet and water *ad libitum*. After Day 14 and for 5 weeks, all mice were fed a high-fat, high-sucrose diet *ad libitum* containing 45% kcal from lipids and 35% kcal from sucrose.

Additionally, each mice from the FMT+BB group was treated daily via orogastric gavage with 0.4g of an aqueous solution of BB extract, containing 0.011 mg of anthocyanins. This BB extract was obtained through the dehydration of BB at 60 °C for 36 hours. For the FMT group, distilled water was administered instead of the extract.

Sample Collection

The animals were euthanized on Day 50 through cervical dislocation after anaesthesia with carbon dioxide (CO_2) inhalation. AT was collected for further analysis.

3T3-L1 Cell Culture as an Adipocyte Model

To study the mechanisms related to mitochondrial function and dynamics at the cellular level in the context of obesity, the cell line of immortalized murine preadipocytes 3T3-L1 was selected, as this cell line is, to date, one of the most widely used cellular models for evaluating processes related to AT and its underlying molecular mechanisms (27, 28). For this purpose, the cells were cultured and then differentiated into adipocytes before applying the treatments required for the different groups. The entire process conducted in the 3T3-L1 cell line culture, from differentiation to treatment, is summarized in Figure 4.

Campo Mártires da Pátria, 130
1169-056 Lisboa · Portugal

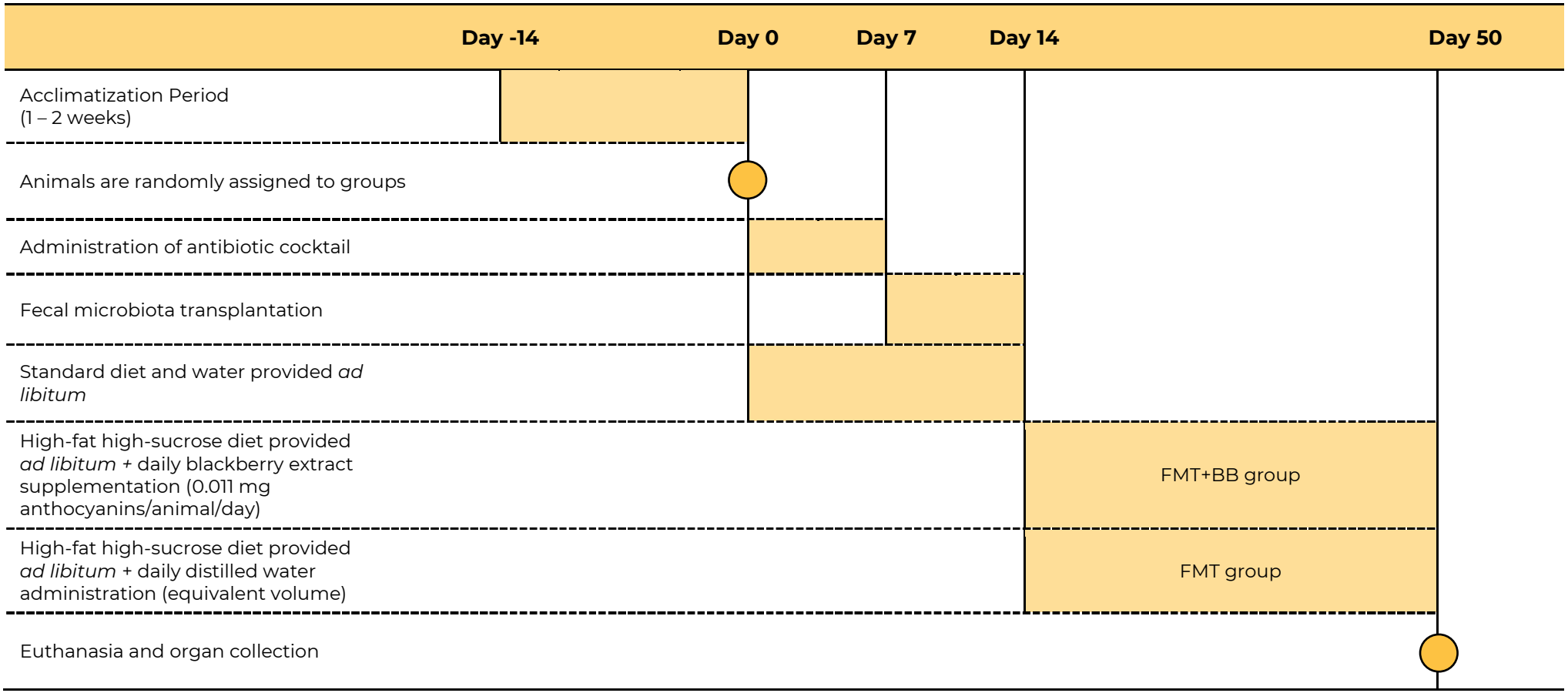

Figure 3. Schematic overview of the MONET study protocol, which includes the acclimatization period, assignment to the two groups (FMT and FMT+BB), treatment, euthanasia and tissue collection.

Campo Mártires da Pátria, 130
1169-056 Lisboa · Portugal

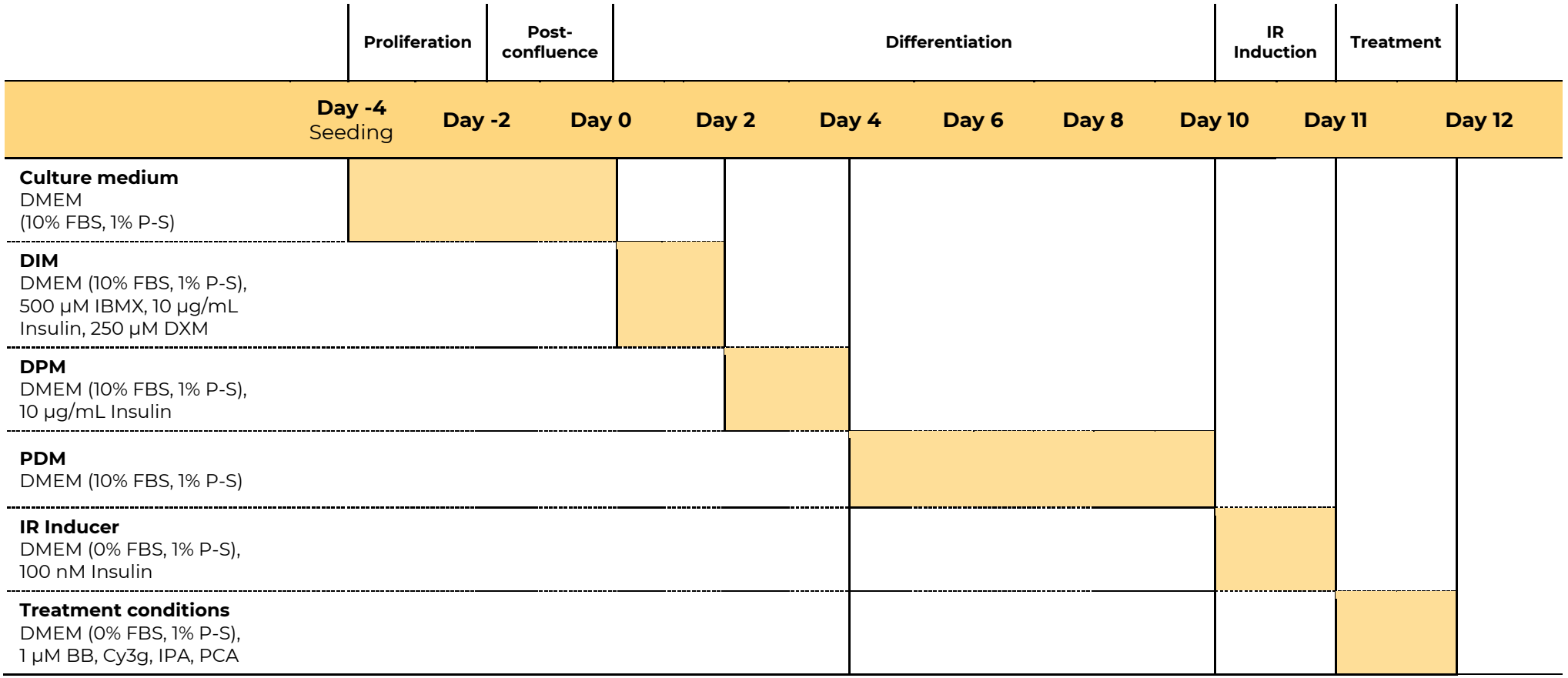

Figure 4. 3T3-L1 protocol timeline. Four days after reaching full confluence (Day 0), 3T3-L1 preadipocytes were incubated with a differentiation induction medium (DIM), consisting of Dulbecco's Modified Eagle's Medium (DMEM) supplemented with 10% fetal bovine serum (FBS), 1% penicillin–streptomycin (P-S), 250 nM dexamethasone (DXM), 10 µg/mL insulin, and 500 µM 3-isobutyl-1-methylxanthine (IBMX). After 2 days (Day 2), DIM was replaced with a differentiation progression medium (DPM), composed of DMEM supplemented (10% FBS, 1% P-S) with 10 µg/mL insulin. On Day 4, the DPM was removed, and cells were subsequently maintained in post-differentiation medium (PDM), consisting of supplemented DMEM (10% FBS, 1% P/S) only. On Day 10, insulin resistance was induced in fully differentiated adipocytes by incubation in unsupplemented DMEM (0% FBS, 1% P-S) containing 100 nM insulin for 24 hours. On Day 11, the medium was replaced with the corresponding treatment condition at 1 µM for 24 hours.

Campo Mártires da Pátria, 130
1169-056 Lisboa · Portugal

Cell Line, Culture Medium Composition and Conditions for Growth and Subculturing

The murine 3T3-L1 preadipocyte cell line from the American Type Culture Collection (ATCC CL-173) was obtained through LGC Promochem (Spain), and was used between passage numbers 6 and 32. Cells were maintained as monolayers in Dulbecco's Modified Eagle's Medium (DMEM), which was supplemented with 1.5 g/L of $NaHCO_3$, 10% (vol/vol) fetal bovine serum (FBS) that had been heat-inactivated at 56°C for 30 minutes, 100 U/mL of penicillin, and 100 U/mL of streptomycin (all reagents from Sigma-Aldrich, Spain). Cultures were incubated at 37°C in a humidified atmosphere of 5% CO_2 and 95% air. The culture medium was renewed every two to three days, and cells were subcultured every three to four days.

For subculturing, cells at approximately 80-90% confluence (estimated visually) were detached using a 0.25% trypsin-ethylenediaminetetraacetic acid solution (Sigma-Aldrich) for five minutes. They were then split at a ratio of 1:3 or 1:5, depending on confluency, and seeded into plastic culture dishes (surface area of 21 cm^2; diameter of 52 mm; Orange Scientific, Belgium).

For the analysis of mitochondrial density, gene expression and protein quantification, cells were seeded into six-well plastic cell culture plates (surface area of 9.6 cm^2; diameter of 34.7 mm; Orange Scientific) that had been previously coated with 0.2% gelatin (Darmstadt, Germany). To quantify ATP synthesis and detect intracellular ROS, cells were seeded into twenty-four-well plastic plates (surface area of 1.93 cm^2; diameter of 16.2 mm; Orange Scientific), coated with gelatin.

Cell Differentiation

Four days after reaching full confluence (designated as Day 0), preadipocytes were exposed to a differentiation initiation medium (DIM) consisting of DMEM as previously described, supplemented with 250 nM dexamethasone (DXM), 10 µg/mL of insulin, and 500 µM 3-isobutyl-1-methylxanthine (IBMX), all from Sigma-Aldrich. On Day 2, this medium was replaced with a differentiation progression medium (DPM), composed of DMEM containing 10 µg/mL of insulin. On Day 4, this medium was replaced with a post-differentiation medium (PDM), consisting solely of DMEM. Cells were used for experiments on Day 10, when more than 80% had fully developed into adipocytes. This was confirmed by microscope images, which showed the change from a fibroblast-like to a round shape and the build-up of lipid droplets (Figure 5).

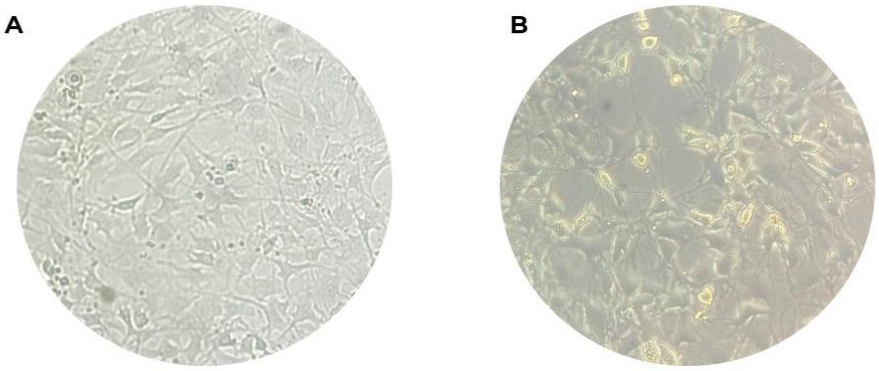

Figure 5. Differentiation of 3T3-L1 preadipocytes into mature adipocytes. Optical microscopy images (40x) were taken prior to media change on selected days. **A:** On Day 3 of differentiation, 3T3-L1 preadipocytes with a fibroblast-like morphology begin to round up and show shortening of their filaments. **B:** On Day 10 of differentiation, cells are fully differentiated into mature adipocytes, showing enlarged lipid droplets.

Insulin Resistance Induction

Ten-day-old differentiated adipocytes were treated for 24 hours with 100 nM insulin (from Sigma-Aldrich) in FBS-free medium to induce IR, as described elsewhere (29). Wells assigned to the negative control group were maintained in DMEM (0% FBS, 1% P-S).

Campo Mártires da Pátria, 130
1169-056 Lisboa · Portugal

Treatment Conditions

Following the purpose of this study, four different treatments were defined: blackberry extract (BB), cyanidin-3-glucoside (C3G), indole-3-propionic acid (IPA) and protocatechuic acid (PCA), all used at a final concentration of 1 µM in DMEM (0% FBS, 1% P-S). Each treatment included 4 replicates (wells).

Stock solutions for all conditions were prepared at 1 mM using filtered DMSO as solvent.

On Day 12 (after 24 hours of insulin treatment to induce IR in differentiated 3T3-L1 adipocytes), cells were treated for an additional 24 hours with one of the above compounds.

Both control (Ø) and IR groups were treated with 1 µM DMSO in DMEM (0% FBS, 1% P-S).

Sample Analysis

Cellular ATP Quantification

After 24 hours of treatment with the different compounds, 3T3-L1 adipocytes were subjected to a luminescent cell viability assay based on the quantification of intracellular ATP. This assay relies on a luciferase-catalyzed reaction, in which luciferin is oxidized in the presence of ATP, Mg^{2+}, and molecular oxygen, resulting in cell lysis and the emission of a luminescent signal. The intensity of this signal is directly proportional to the amount of ATP and, consequently, to the number of metabolically active cells.

The kit used was the CellTiter-Glo® 2.0 Assay from Promega. Following the manufacturer's protocol, the kit reagent (with thermostable luciferase and Mg^{2+}) was added to the treated cells. The dilution used in culture medium was 1:5, and it was chosen based on preliminary observations indicating that various reagent-to-medium ratios have proportional luminescent signals across all conditions. More precisely, 1:2 ratio generated signals beyond the calibration curve range, whereas the 1:5 ratio remained within measurable limits.

After mixing for 2 minutes using an orbital shaker to ensure complete cell lysis, 100 µL from each well was transferred to a black 96-well plate. The plate was then incubated at room temperature for 10 minutes to allow stabilization of the luminescent signal. Luminescence was recorded using a Tecan Spark Multimode Microplate Reader, allowing quantification of ATP levels in the samples.

Intracellular ROS Detection

To assess intracellular levels of ROS, a fluorescence-based assay using the 2',7'-dichlorodihydrofluorescein diacetate (DCFH-DA) probe was performed, as described by Kim et al (30). DCFH-DA is a non-fluorescent, cell-permeable compound that, upon entering the cell, is hydrolyzed by intracellular esterases to 2',7'-dichlorodihydrofluorescein (DCFH). In the presence of ROS, DCFH is oxidized to 2',7'-dichlorofluorescein (DCF), a fluorescent molecule that emits green light at 530 nm when excited at 485 nm.

After the 24-hour treatment period, adherent 3T3-L1 cells were incubated with a DCFH-DA working solution (prepared by diluting a 10 mM stock solution in pre-warmed DMEM without FBS) at 37 °C for 30 minutes. Following incubation, the DCFH-DA working solution was removed, cells were washed once with PBS and lysed with 0.1% Triton X-100 in Tris buffer. After a 5-minute incubation at room temperature, cell lysates were collected into 1.5 mL tubes and centrifuged at 21,130 × g for 5 minutes at 4 °C. Afterwards, 100 µL of supernatant from each tube was transferred to a black 96-well plate, and fluorescence intensity was measured using a Tecan Spark Multimode Microplate Reader under predefined conditions (excitation 485 nm, emission 530 nm).

To normalize the obtained ROS fluorescence signals, total protein content in each sample was determined using the EZQ® Protein Quantitation Kit (ThermoFisher). A standard curve of ovalbumin was generated, allowing the calculation of each sample's total protein concentration based on its fluorescence value. ROS levels, previously measured, were then normalized to the corresponding protein content.

DNA Extraction

Genomic DNA was extracted from 50 mg of AT using the QIAamp Fast DNA Tissue Kit (QIAGEN), following the manufacturer's instructions. Tissue samples were homogenized in Tissue Disruption Tubes with a digestion buffer containing Proteinase K and RNase A and incubated at 56 °C for 1 hour

Campo Mártires da Pátria, 130
1169-056 Lisboa · Portugal

with agitation. After lysis, Buffer MVL was added, and lysates were transferred to silica spin columns. DNA was purified through successive washes with Buffers AW1 and AW2, and eluted in 50 µL of Buffer ATE.

Genomic DNA was also isolated from 3T3-L1 cells using the NZY Tissue gDNA Isolation Kit (NZYtech, MB135), following the manufacturer's protocol. Cells were resuspended in Buffer NT1, to which Proteinase K and Buffer NL were added. After a 10–15 min incubation at 56 °C, ethanol was added to the lysate. The mixture was applied to a silica spin column and washed with Buffers NW1 and NW2. DNA was then eluted in 100 µL of Buffer NE at 70 °C.

Genomic DNA content of all samples was measured using the Nanodrop 200 and then stored at -20 °C.

Mitochondrial Density Analysis

The estimation of mtDNA copy number was performed by quantitative real-time PCR (qPCR), following the protocols established by Quiros et al. (31) and Guo et al (32). Both authors state that, in the same way that cells contain two copies of each chromosome, nDNA to mtDNA ratios can also be determined, allowing for the calculation of mtDNA copy number.

For the genomic DNA extracted from AT, qPCR was performed using the following components: 2.5 µL of genomic DNA at a concentration of 40 ng/µL, 0.5 µL of each primer (forward and reverse), 5 µL of SYBR Green Mix, and 1.5 µL of Milli-Q water, making a total of 10 µL per well. For these samples, two nuclear genes (Hexokinase 2 (HK2) and NDUFV1) and two mitochondrial genes (ND1 and cytochrome c oxidase subunit I (CO1)) were assessed.

Table 1. Description of target genes and primer sequences used for qPCR analysis of mitochondrial density.

Gene symbol	Gene name	Gene function	Primer sequence (5' -> 3')	Annealing temperature (°C)
HEK2	Hexokinase 2	Key glycolytic enzyme; nuclear-encoded gene involved in glucose metabolism and insulin signaling	F: CCGGCTGCGTATTCTACGTT R: GGGAACACAAAAGACCTCTTCTGG	63
NDUFV1	NADH:Ubiquinone Oxidoreductase Core Subunit V1	Core subunit of mitochondrial Complex I; nuclear-encoded gene responsible for electron transfer from NADH to ubiquinone	F: CTTCCCCACTGGCCTCAAG R: CCA AAA CCC AGT GAT CCA GC	63
ND1	Mitochondrially Encoded NADH:Ubiquinone Oxidoreductase Core Subunit 1	Subunit of mitochondrial Complex I; mitochondrial-encoded gene essential for electron transport and proton pumping	F: CTAGCAGAAACAAACCGGGC R: CCGGCTGCGTATTCTACGTT	63
CO1	Mitochondrially Encoded Cytochrome C Oxidase Subunit 1	Catalytic subunit of mitochondrial Complex IV; mitochondrial-encoded gene transferring electrons from cytochrome c to oxygen	F: TGCTAGCCGCAGGCATTAC R: GGGTGCCCAAAGAATCAGAAC	63

For the genomic DNA extracted from 3T3-L1 cells, qPCR was performed using the following components: 10 µL of genomic DNA at a concentration of 5.5 ng/µL, 0.5 µL of each primer (forward and reverse) and 9 µL of SYBR Green Mix, making a total of 20 µL per well. For these samples, one nuclear gene (HK2) and one mitochondrial gene (ND1) were assessed.

For all samples, the qPCR conditions were equal: (pre-amplification step) 95°C for 5 min, (amplification step) 45 cycles of 95°C for 10 s, 63°C for 10 s and 72°C for 20 s. Finally, a melting curve was calculated to confirm the presence of a single PCR product following these steps: 95°C for 1 s, 70°C for 20 s and 95°C for 1 s.

Campo Mártires da Pátria, 130
1169-056 Lisboa · Portugal

The formulas used to calculate the number of mtDNA copies per sample are shown below:

(1) $\Delta Ct = Ct(nDNA\ gene) - Ct(mtDNA\ gene)$

(2) $Copies\ of\ mtDNA = 2 \times 2^{\Delta Ct}$

RNA Extraction and cDNA Synthesis

Total RNA was extracted from approximately 50 mg of AT using NZYol reagent (NZYTech). Tissue samples were homogenized in 600 µL of NZYol with ceramic beads by vortexing horizontally for 10 minutes. The lysates were transferred to clean 1.5 mL microtubes, including tissue debris when present. Chloroform (200 µL per 1 mL of NZYol) was added, vortexed for 15 seconds, and incubated at room temperature for 15 minutes. The tubes were then centrifuged at 12,000 × g for 15 minutes at 4 °C, and the aqueous (upper) phase was carefully transferred to a new tube, avoiding contamination from the interphase. RNA was precipitated with isopropanol (500 µL per 1 mL of NZYol), incubated for 10 minutes at room temperature, and centrifuged at 12,000 × g for 10 minutes at 4 °C. The pellet was washed with 75% ethanol (in DEPC-treated water), vortexed, and centrifuged at 7,500 × g for 5 minutes at 4 °C. After discarding the supernatant, the RNA pellet was incubated at 60 °C until completely dry. Finally, the RNA was resuspended in DEPC-treated water by pipetting up and down until fully dissolved.

Total RNA was also extracted from cultured cells using NZYol reagent (NZYTech), following the protocols described before.

RNA content of all samples was measured using the Nanodrop® 200.

cDNA was synthesized using a PCR Bio-Rad T100 Thermal Cycler and a mix of 8 µL of sample containing 1 µg of total RNA, 10 µL of NZYRT 2× Master Mix and 2 µL of NZYRT Enzyme Mix (NZY First-Strand cDNA Synthesis Kit; NZYTech; Cat. No. MB125). This mixture was incubated 10 minutes at 25 °C, 30 minutes at 50 °C and 5 minutes at 85 °C. Afterwords, 1 µL of NZYRNase H was added to each tube and incubated by 20 minutes at 37 °C and 5 minutes at 85 °C. To finalize, 21 µL of Milli-Q water was added to each tube, resulting in a final concentration of 25 ng cDNA/µL.

Gene Expression Analysis

The analysis of the expression of important markers of mitochondrial function and activity was conducted through the qPCR of the cDNA previously synthesized.

The genes assessed in the AT samples were CIDEA, PGC1α, Dio2, PPARα, PPARγ, TMEM26, and UCP1, while those assessed in the 3T3-L1 samples were PGC1α, PPARγ, UCP1, MCP1, and AhR.

For all genes, qPCR was performed using the following components: 2.5 µL of cDNA at a concentration of 25 ng/µL, 0.5 µL of each primer (forward and reverse), 5 µL of SYBR Green Mix, and 1.5 µL of Milli-Q water, making a total volume of 10 µL per well. qPCR conditions were similar for all genes, with variations only in the annealing and extension temperatures. The program was as follows: (pre-amplification step) 95°C for 5 minutes; (amplification step) 45 cycles of 95°C for 10 seconds, annealing temperature for 10 seconds, and 72°C for 20 seconds. Finally, a melting curve was generated to confirm the presence of a single PCR product, with the following steps: 95°C for 1 second, 69–72°C for 20 seconds, and 95°C for 1 second. At the end, the expression of all genes was normalized to HPRT.

Campo Mártires da Pátria, 130
1169-056 Lisboa · Portugal

Table 2. Description of target genes and primer sequences used for qPCR analysis of marker of mitochondrial function.

Gene symbol	Gene name	Gene function	Primer sequence (5' -> 3')	Annealing temperature (°C)
HPRT	Hypoxanthine Phosphoribosyltransferase	Nuclear-encoded gene; enzyme in purine salvage pathway; widely used as a housekeeping gene in qPCR	F: GCCCCAAAATGGTTAAGGTT R: CAAGGGCATATCCAACAACA	58
CIDEA	Cell Death Inducing DFFA Like Effector A	Nuclear-encoded gene; lipid droplet-associated protein, promotes lipid storage and regulates thermogenesis in brown/beige adipose tissue	F: GGCCGTGTTAAGGAATCTGC R: GTATGTGCCCGCATAGACCA	60
PGC1α	Peroxisome Proliferator-Activated Receptor Gamma Coactivator 1 Alpha	Nuclear-encoded gene; master regulator of mitochondrial biogenesis and oxidative metabolism; coactivates PPARs and other transcription factors	F: TGGATGAAGACGGATTGCCC R: AGAGCTTCTTAAGTAGAGACGGC	60
Dio2	Type II Iodothyronine Deiodinase	Nuclear-encoded gene; enzyme that converts thyroxine (T4) into active triiodothyronine (T3), essential for thermogenic activation of brown/beige adipocytes	F: CTTCTGAGCCGCTCCAAGTC R: CCCAGTTTAACCTGTTTGTAGGC	59
PPARα	Peroxisome Proliferator-Activated Receptor Alpha	Nuclear-encoded gene; nuclear receptor that regulates fatty acid oxidation and lipid metabolism	F: CCCTGAACATCGAGTGTCGAA R: TTCGCCGAAAGAAGCCCTTA	62
PPARγ	Peroxisome Proliferator-Activated Receptor Gamma	Nuclear-encoded gene; nuclear receptor critical for adipocyte differentiation, lipid storage, and insulin sensitivity	F: GGTGTGATCTTAACTGCCGGA R: GCCCAAACCTGATGGCATTG	62
TMEM26	Transmembrane Protein 26	Nuclear-encoded gene; surface marker of beige adipocytes, associated with thermogenic capacity	F: GAAACCAGTATTGCAGCACCC R: CCCATTCCATTGGTGGCTCT	62
UCP1	Uncoupling Protein 1	Mitochondrial-encoded gene; protein in the inner mitochondrial membrane that uncouples oxidative phosphorylation, generating heat (non-shivering thermogenesis)	F: ATACTGGCAGATGACGTCCC R: GGTACGCTTGGGTACTGTCC	61

Protein Collection

Proteins were extracted from 3T3-L1 cells using RIPA lysis buffer (Boster Biological Technology) containing a protease inhibitor cocktail (Sigma, P8340; dilution 1:50). Cell monolayers were rinsed three times with 1 mL of ice-cold PBS, and resuspended in 1 mL lysis buffer. The lysates were aliquoted and stored at −80 °C until further analysis.

Mitochondrial Dynamics Assessment

To assess variations among the different groups of 3T3-L1 cells in key mitochondrial dynamics processes, the levels of the following proteins were quantified by Western blot: Mitofusin-2

Campo Mártires da Pátria, 130
1169-056 Lisboa · Portugal

(mitochondrial fusion), DRP1 (mitochondrial fission), PGC1α (mitochondrial biogenesis) and Parkin (mitophagy). Cell lysates were resuspended 1:2 (v/v) in a mixture of Laemmli sample buffer (Bio-Rad) and beta-mercaptoethanol (Millipore-Sigma), and this mixture was heated at 100°C for 10 min to denature proteins. Twenty to thirty micrograms of protein/sample were loaded onto 4-15% precast polyacrylamide gels (Bio-Rad) and proteins were separated by electrophoresis and transferred to nitrocellulose membranes (GE Healthcare–Amersham Biosciences, United Kingdom) using a wet transfer method (Bio-Rad) for 95 minutes at 100 V in a cold environment. Membranes were then blocked for 1 hour at room temperature in PBS containing 0.1% (v/v) Tween-20 (TPBS) and 5% (w/v) skimmed milk powder (Molico, Nestlé, Switzerland). After blocking, membranes were incubated overnight at 4 °C with the appropriate primary antibodies, following the supplier's instructions. After incubation, membranes were washed three times for 10 minutes in TPBS, then incubated for 1 hour with gentle shaking with the appropriate secondary antibody, again following supplier instructions. Membranes were washed again (3 × 10 minutes) in TPBS. The proteins of interest were then visualized by chemiluminescence using the ChemiDoc™ Touch Imaging System (Bio-Rad), after incubation with *SuperSignal™ West Pico PLUS substrate* (Thermo Fisher Scientific, USA) for 3 – 3.5 minutes. The relative band densities of each protein were quantified using Fiji software (version 2.9.0/1.53t) and expressed as a ratio relative to GAPDH.

Statistical Analysis

Statistical analysis was performed using GraphPad Prism version 10.0.0 (GraphPad Software, USA). Data are presented as mean ± standard error of the mean (SEM). *n* represents the number of replicate wells analysed per treatment. For comparisons between two groups, unpaired two-tailed Student's t-test was used. When more than two groups were analysed, one-way ANOVA was performed, followed by Brown-Forsythe and Bartlett's tests to assess homogeneity of variances. Differences were considered statistically significant when $p < 0.05$.

Campo Mártires da Pátria, 130
1169-056 Lisboa · Portugal

Results

Blackberry Supplementation Increases Mitochondria Content in Mice Adipose Tissue

Mitochondrial DNA was evaluated in AT through qPCR. In Figure 6, a significant increase in mtDNA copy number can be seen in the group supplemented with BB (FMT+BB) compared to the FMT group ($p < 0.01$).

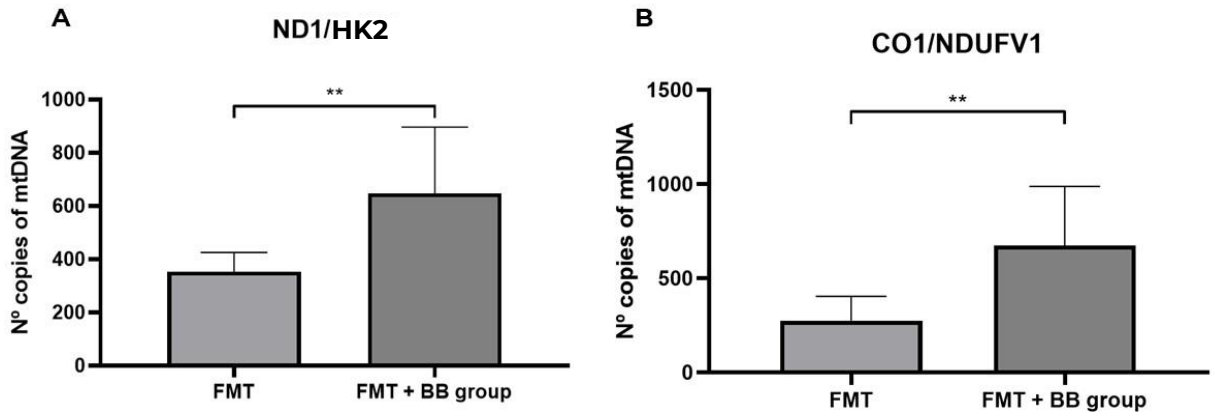

Figure 6. Mitochondrial DNA (mtDNA) copy number in adipose tissue under different treatment conditions. Values represent the average of the ratio mtDNA/nDNA copy numbers calculated by ND1/HK2 (Figure 6A) and CO1/NDUFV1 (Figure 6B) gene ratios. Experimental groups include mice subjected to a high-fat diet plus fecal microbiota transplantation (FMT), and high-fat diet plus FMT and blackberry extract (FMT+BB). Each bar represents the mean ± SD (n=7-8). **$p < 0.01$.

Blackberry Supplementation Potentially Enhances Thermogenesis in Mice Adipose Tissue

Through qPCR of cDNA extracted from visceral AT, it was possible to evaluate the expression of relevant genes for the metabolic activity of adipocytes. Table 3 shows data indicating that there are no significant differences between the groups (FMT vs. FMT+BB) for any of the genes analyzed (mCIDEA, mPGC1α, mDio2, mPPARα, mPPARγ, mTMEM26, mUCP1). However, it is still interesting to note an apparent trend related to thermogenesis genes, *i.e.* an increased expression of TMEM26, UCP1, and Dio2 in the in the FMT+BB compared with the FMT group.

Table 3. Relative gene expression of mCIDEA, mPGC1α, mDio2, mPPARα, mPPARγ, mTMEM26, and mUCP1 in subcutaneous adipose tissue, across the experimental groups: Fecal Microbiota Transplantation (FMT), and FMT supplemented with blackberry extract (FMT+BB). Expression was normalized with HPRT expression. Data are expressed as mean Cq (SD).

	FMT (n = 36)	FMT+BB (n = 36)	p Value
mCIDEA	0.007 (0.008)	0.008 (0.004)	0.841
mPGC1α	0.018 (0.018)	0.006 (0.002)	0.157
mDio2	0.018 (0.026)	0.045 (0.088)	0.442
mPPARα	0.003 (0.003)	0.001 (0.002)	0.418
mPPARγ	0.149 (0.058)	0.128 (0.074)	0.623
mTMEM26	0.003 (0.006)	0.005 (0.007)	0.673
mUCP1	0.003 (0.004)	0.010 (0.014)	0.266

Campo Mártires da Pátria, 130
1169-056 Lisboa · Portugal

BB, C3G, IPA, and PCA Treatments Reduce ATP Content in Insulin-Resistant 3T3-L1 Cells

Mitochondria in white adipocytes are the main source of ATP production, which is essential to sustain the metabolic activity of cells and tissues (33). Based on this, it is reasonable to assume that a more metabolically active cell would produce higher levels of ATP.

Insulin-resistant adipocyte cell model was treated with BB extract, the main anthocyanin present C3G, IPA and PCA, which are microbiota' and anthocyanin' metabolites respectively, and ATP production was evaluated. In Figure 7 it is presented the average ATP concentration measured in each study group. An increase in ATP concentration was observed in the group with IR alone, compared to the control. Conversely, a decrease in ATP concentration was observed in the groups with IR treated with BB, C3G, IPA and PCA.

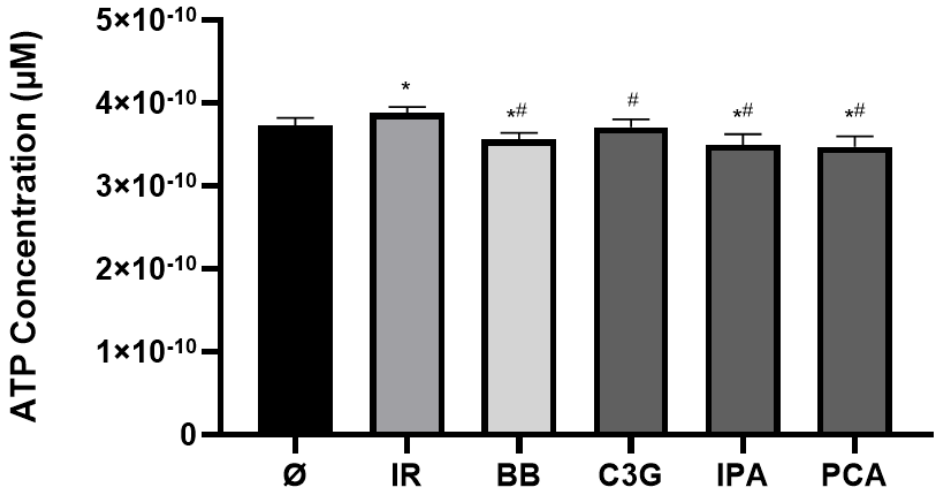

Figure 7. ATP concentration (µM) in 3T3-L1 adipocytes under different experimental conditions. Groups include untreated control cells (Ø), insulin resistant (IR) cells, and IR cells treated with either blackberry (BB), cyanidin-3-glucoside (C3G), indole-3-propionic acid (IPA), or protocatechuic acid (PCA), all used at a final concentration of 1 µM in DMEM (0% FBS, 1% P-S). Each bar represents the mean ± SD (n=4). *p < 0.05 vs control (Ø); #p < 0.05 vs IR.

ROS Levels Are Not Altered in Insulin-Resistant 3T3-L1 Adipocytes After BB, C3G, IPA, or PCA Treatment

It is known that obesity relates with oxidative stress in AT, including elevated ROS levels (34). In Figure 8, it is possible to observe that ROS levels did not significantly differ across groups (Ø, IR, BB, C3G, IPA, PCA), but there is a trend towards lower ROS production in IR adipocytes and a slight increase upon treatment (BB, C3G, IPA, or PCA).

Campo Mártires da Pátria, 130
1169-056 Lisboa · Portugal

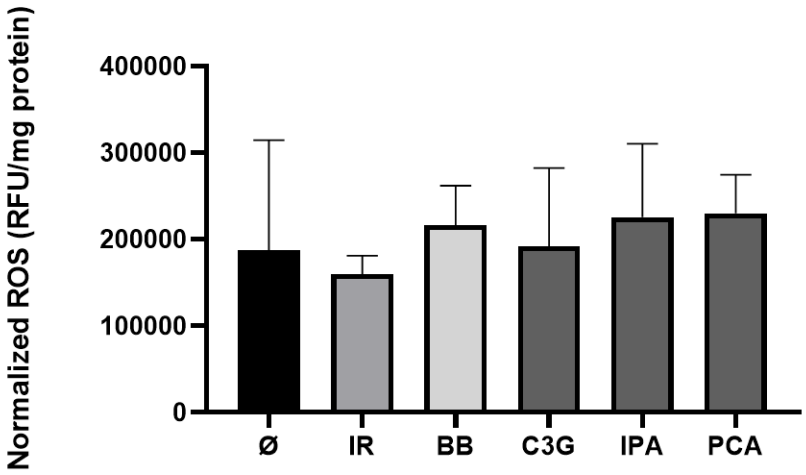

Figure 8. Intracellular ROS levels normalized to total protein content (expressed as RFU per mg protein) in 3T3-L1 adipocytes under different experimental conditions. Groups include untreated control cells (Ø), insulin resistance (IR) cells, and IR cells treated with either blackberry (BB), cyanidin-3-glucoside (C3G), indole-3-propionic acid (IPA), or protocatechuic acid (PCA), all used at a final concentration of 1 µM in DMEM (0% FBS, 1% P-S). Data are presented as mean ± SD (n=3-4).

Blackberry Anthocyanin Modulates Mitochondrial Content in 3T3-L1 cells

The mtDNA in 3T3-L1 cells was evaluated through qPCR. In Figure 9, the mtDNA copy number is expressed as the gene ratio of ND1 to HK2. A reduction in mtDNA copy number induced by C3G compared to control conditions was observed, as well as an increase induced by IPA compared to IR.

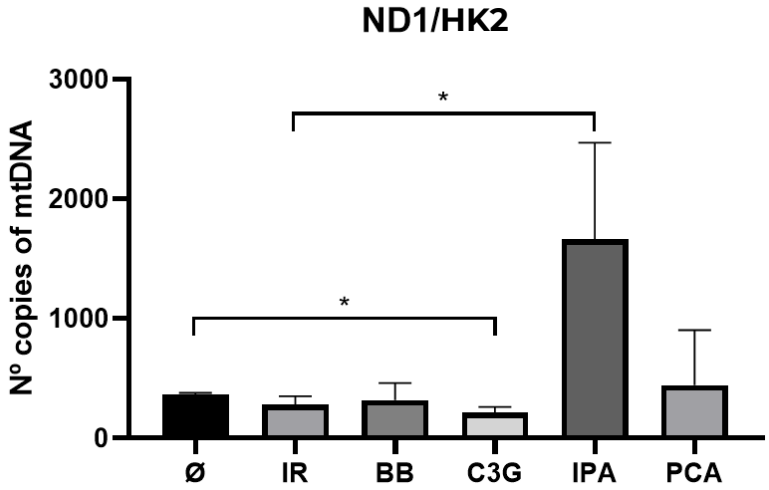

Figure 9. mtDNA copy number in 3T3-L1 cell line under different experimental conditions. Groups include untreated control cells (Ø), insulin resistance (IR) cells, and IR cells treated with either blackberry (BB), cyanidin-3-glucoside (C3G), indole-3-propionic acid (IPA), or protocatechuic acid (PCA), all used at a final concentration of 1 µM in DMEM (0% FBS, 1% P-S). Data are presented as mean ± SD (n=2-4).

Campo Mártires da Pátria, 130
1169-056 Lisboa · Portugal

Insulin Resistance Disrupts Mitochondrial Dynamics, While PCA Partially Restores Fusion and Fission in 3T3-L1 Cells

Western blot analysis allowed us to assess differences in key mitochondrial dynamic processes within the established groups (Ø, IR, BB, C3G, IPA, PCA), more precisely at the level of mitochondrial fusion (via mitofusin-2), mitochondrial fission (DRP-1), mitochondrial biogenesis (PGC1α) and mitophagy (Parkin).

Figures 10A, 10B1, 10C1, 10D1 and 10E1 show Western blot bands for the analyzed proteins across experimental groups, while Figures 10B2, 10C2, 10D2 and 10E2 present the corresponding quantification plots, illustrating variations in protein expression and related mitochondrial processes.

Figures 10B1 and 10B2 shows that mitofusin-2 expression was significantly reduced in IR cells compared to control conditions, indicating impaired mitochondrial fusion in IR, while PCA treatment partially reversed this effect.

Similarly, in Figures 10C1 and 10C2, we observed that DRP-1 protein levels were significantly increased in the PCA group compared to the IR group.

In Figures 10D1 and 10D2, PGC1α, a regulator of mitochondrial biogenesis, was significantly decreased in the IR group compared to the control. This reduction was further observed in all treatments except PCA, highlighting that both IR and bioactive compound supplementation can modulate mitochondrial biogenesis.

Regarding Parkin protein levels (Figures 10E1 and 10E2), they remained unchanged across all groups, indicating that mitophagy may not be significantly affected under these conditions.

Altogether, these results suggest that IR disrupts mitochondrial fusion and biogenesis, while treatments, particularly with PCA, appear to restore or modulate fusion and fission processes.

Campo Mártires da Pátria, 130
1169-056 Lisboa · Portugal

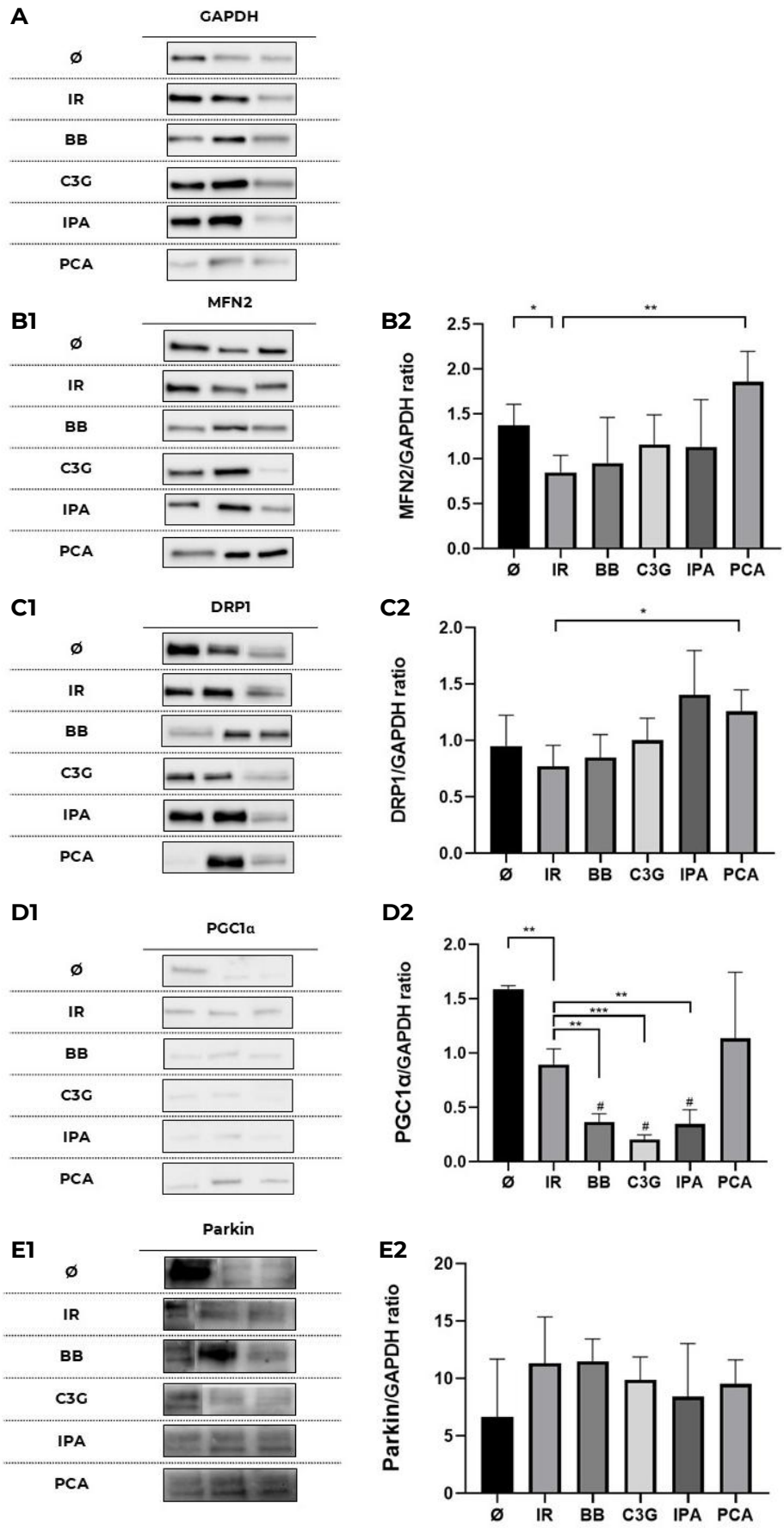

Figure 10. Expression of key proteins involved in mitochondrial dynamics across experimental groups. (A, B1, C1, D1, E1) Western blot images for each group (three replicates per group) and for each protein analyzed (GAPDH, MFN2, DRP1, PGC1α, Parkin). (B2, C2, D2, E2) Quantification of protein expression, calculated as the ratio of target protein band intensity to GAPDH, for: (B2) Mitofusin-2 (fusion), (C2) DRP-1 (fission), (D2) PGC1α (biogenesis), and (E2) Parkin (mitophagy). Groups include untreated control cells (Ø), insulin resistance (IR) cells, and IR cells treated with either blackberry (BB), cyanidin-3-glucoside (C3G), indole-3-propionic acid (IPA), or protocatechuic acid (PCA), all used at a final concentration of 1 µM in DMEM (0% FBS, 1% P-S). Data are expressed as mean ± SEM (n=3-4). *p value < 0.05, ** p value < 0.01, *** p value < 0.001, # p value < 0.0001 vs. control group (Ø).

Campo Mártires da Pátria, 130
1169-056 Lisboa · Portugal

BB And PCA Modulate Thermogenesis and Mitochondrial Biogenesis in 3T3-L1 cells

Figure 11 presents the relative gene expression levels of selected target genes related to mitochondrial function (mUCP1 and mPGC1α) in differentiated 3T3-L1 adipocytes across experimental conditions. Regarding the impact of IR, an increase in UCP1 expression is observed, which is counterbalanced by the different treatments applied (BB and PCA). This contradictory effect between IR and a treatment is also noticed for mPGC1α, but in this case only for C3G and in an opposite way: a tendency for decreased expression in IR compared to control conditions, but a significant increase in C3G *vs.* control conditions.

The expression of the remaining genes studied (mPPARγ, mMCP1, and AhR) did not show significant differences between the control and any of the treatment groups (Table S1). In general, mPPARγ and mMCP1 expression levels remained stable across all comparisons, while AhR expression showed a trend toward higher values in the BB and C3G groups.

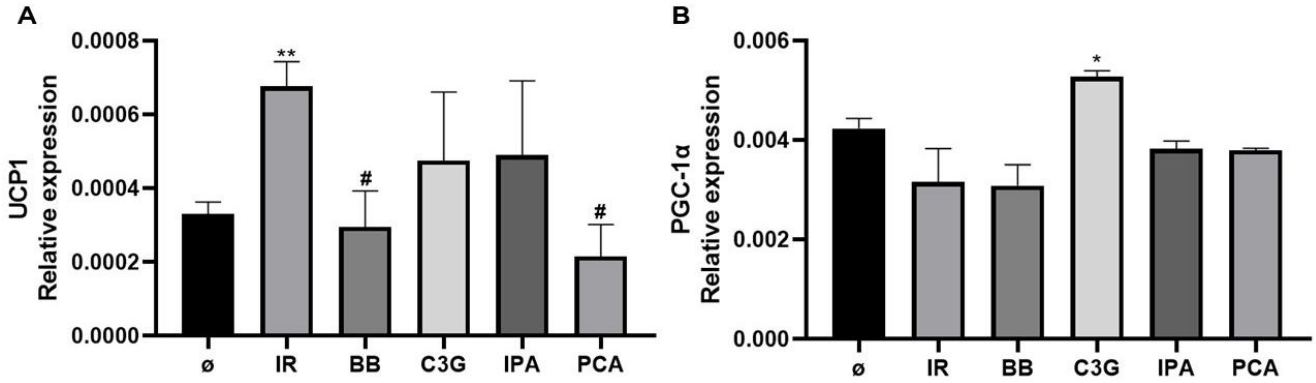

Figure 11. Relative expression of genes related to mitochondrial function in differentiated 3T3-L1 adipocytes, across experimental groups. A: mUCP1; **B:** mPGC1α. Gene expression normalized with HPRT. Groups include untreated control cells (Ø), insulin resistance (IR) cells, and IR cells treated with either blackberry (BB), cyanidin-3-glucoside (C3G), indole-3-propionic acid (IPA), or protocatechuic acid (PCA), all used at a final concentration of 1 µM in DMEM (0% FBS, 1% P-S). Data are expressed as mean Cq (SD) (n=3-4). *p value < 0.05 vs Ø. ** p value < 0.005 vs Ø. # p value < 0.05 vs IR.

Campo Mártires da Pátria, 130
1169-056 Lisboa · Portugal

Discussion

Mitochondria are organelles found in eukaryotes that are essential for energy metabolism and cellular homeostasis, and which dysfunction has been constantly linked to the pathogenesis of obesity (35). Therefore, it is important to learn about this organelle under obesity conditions and explored them as a target for novel therapeutic approaches.

Over the last years, polyphenols, and more importantly anthocyanins, have been recognized as potential adipocyte metabolism and mitochondrial function regulators (36, 37, 38).

According to such context, the present work aimed to investigate the impact of BB supplementation and its major anthocyanin component, C3G, and microbial metabolites, PCA and IPA, on mitochondrial function in obesity. The approach used considered of two models: (i) *in vivo*, through analysis of AT samples from the MONET pre-clinical trial, where the impact of BB supplementation was tested using a diet-induced model of obesity in humanized mice through human FMT; and (ii) *in vitro*, using 3T3-L1 adipocytes with IR, treated with BB extract or with isolated compounds.

Blackberry Supplementation in Mice Adipose Tissue

We observed that BB supplementation significantly altered mtDNA copy number in AT compared to the control (unsupplemented) group. Since mtDNA copy number is generally accepted to be a marker for mitochondrial content and biogenesis, the observation here shows that consumption of blackberry increases mitochondrial content. This agrees with previous research demonstrating anthocyanin-high diet increases markers of mitochondrial biogenesis, including PGC1α (39).

To note that the mtDNA copy number increase was not coupled with statistically significant gene expression modifications for biogenesis markers like PGC1α. This apparent contradiction calls for some some considerations. The mtDNA content will not always be accompanied by transcriptional regulation at the point of measurement. Biogenesis is a dynamic process and transcriptional activators such as PGC1α would be anticipated to produce transient peaks, not found at some arbitrary time point (40). So, biogenesis could have occurred earlier with supplementation and the mtDNA increase at the tissue level as a residual effect maintained after transcriptional upregulation.

No significant alterations on the expression of genes for thermogenesis were observed in control AT samples, but a rising trend in TMEM26, UCP1, and Dio2 gene expression was noticed in the BB-supplemented group. These genes are most often associated with white adipose browning, an energy-enhancing process via activation of thermogenesis (41). Even transient stimulation of thermogenic markers can improve energy balance, as demonstrated in models where activation of Dio2 or UCP1 led to an increase in whole-body oxygen consumption (42, 43). Over the long term, such increases in energy dissipation may shift the energy balance away from fat storage, thereby limiting weight gain and improving metabolic outcomes (44). Thus, mild browning responses could be an important mechanism to switch the trajectory of obesity.

Together, these findings support the idea that BB supplementation favours mitochondrial adaptation of AT by increasing mitochondrial content. Although the exact mechanisms remain unclear, there have been multiple plausible explanations that can be derived from the literature. Anthocyanins and their metabolites have been reported to stimulate mitochondrial biogenesis and oxidative pathways (45, 46), enable antioxidant protection against ROS accumulation, and modulate the gut microbiota, whose metabolic products might also have a systemic impact. Therefore, studies have to target not only BB supplementation *per se*, but also the anthocyanin constituents and their metabolites.

BB, C3G, PCA and IPA Supplementation on 3T3-L1 Adipocytes

To support the *in vivo* results, 3T3-L1 differentiated adipocytes were used as this is a model widely used to study adipocytes biology (25, 27, 28, 29). IR was either induced or not, in order to mimic a metabolic feature of obesity, and cells were subsequently treated with different compounds (BB, C3G, PCA, and IPA). Based on the available literature, the following parameters were selected to have a comprehensive view of mitochondrial function: ATP production, ROS levels, mitochondrial content, and specific genes and protein expression related to mitochondrial function (6, 23, 42, 43, 44).

Campo Mártires da Pátria, 130
1169-056 Lisboa · Portugal

ATP is the primary energy unit of the cell, essential to sustain most biological processes. Under physiological conditions, ATP is predominantly produced in the mitochondria through oxidative phosphorylation, making its quantification a relevant parameter to monitor mitochondrial function (47).

It was expected to obtain a lower ATP concentration in the IR group, as it is a feature of obesity, and an increased ATP concentration with treatments (33). However, our results showed increased ATP production in the IR group, followed by a reduction with all treatment. This suggests that, despite the unfavourable environment of IR, cells promote ATP production through alternative pathways. More precisely, a plausible explanation is a metabolic switch from oxidative phosphorylation to compensatory glycolysis, a mechanism similar to the Warburg effect of cancer cells (47). In Yang C et al it was shown that insulin exposure (e.g., 100 nM for 48h) can induce mitochondrial uncoupling, leading to increased oxygen consumption without losing the function of ATP production (48). Consequently, ATP content increases in IR cells, not due to enhanced mitochondrial activity, but due to glycolytic compensation. All treatment groups show decreased ATP levels, which can be due improved mitochondrial coupling and suppression of this compensatory mechanism.

Considering that obesity is generally associated with increased oxidative stress (9, 10), it could be expected that ROS levels would be elevated in the IR group and diminished in the treatment groups. However, this was not observed. Although not statistically significant, our findings are consistent with the ATP results, as IR cells showed a tendency toward reduced ROS levels compared with control, while treatments resulted in higher ROS levels relative to IR. Reduced ROS in IR adipocytes could reflect decreased electron flux through the electron transport chain, consistent with impaired oxidative metabolism and reliance on glycolysis. Treatment with BB, C3G, PCA, and IPA slightly increased ROS levels, which is indicative of reactivation of mitochondrial respiration. Thus, the ROS pattern observed here supports the hypothesis that treatments re-adjust the energy metabolism in the mitochondria, shifting cells away from glycolytic compensation.

When assessing mitochondrial content, we observed treatment-specific effects: IPA increased mtDNA compared to IR cells, whereas C3G reduced it compared to control (Ø). PCA showed a slight, upward trend, and whole BB had no effect. These contrasting outcomes highlight that anthocyanins and their metabolites do not act on the same targets or by the same mechanisms.

The increase in mtDNA with IPA points to a stimulation of mitochondrial biogenesis or protection of mtDNA integrity. Previous work has shown IPA to be a strong antioxidant capable of upregulating genes involved in mitochondrial maintenance, such as SIRT1 (49). Regarding C3G, it was not expected to be reduced, since anthocyanins are usually thought to promote biogenesis. One possible explanation is that, as mitochondrial efficiency improves, cells may not need as many mitochondria, leading to a lower steady-state mtDNA content. In the end, these opposite effects of C3G and IPA illustrate the complexity of anthocyanin metabolism, where compounds and their metabolites can act through very different mechanisms.

Gene and protein expression were evaluated by qPCR and Western blot, respectively, to search for differences in key mitochondrial processes.

Western blotting revealed important data on mitochondrial fission/fusion dynamics. IR reduced expression of MFN2, consistent with impaired fusion capacity. It has been reported that impaired mitochondrial fusion is usually counterbalanced by the promotion of mitochondrial fission, and vice versa (50). However, our model reveals another side of these processes: a clear decrease in fusion (as observed in the IR group) can occur without a compensatory increase in fission. This suggests that IR may reduce overall mitochondrial dynamics, rather than merely shifting the fission/fusion balance.

Additionally, PCA treatment increased significatively, with regards to IR group, MFN2 (fusion) and DRP1 (fission). As a balanced fission and fusion are central to maintaining mitochondrial quality, and disruptions in this process are intimately linked to IR (51), having a metabolite (PCA) restoring it is an important finding. The remaining treatments, even though without significative difference, follow the same trend as PCA (increased expression of MFN2 and DRP1 in comparison with IR).

Campo Mártires da Pátria, 130
1169-056 Lisboa · Portugal

Regarding protein content, the expression of PGC1α, involved in mitochondrial biogenesis, decreased in all groups (IR, BB, C3G, IPA) compared with baseline, except PCA. Additionally, it is important to remember that in IPA it was observed an increased in mitochondrial content. This apparent discrepancy between decreased PGC1α expression and increased mtDNA copy number in the IPA group may be explained by the fact PGC1α activity is also transient and dose-dependent, with early peaks (2–8 h) that may not reflect total levels at 24–48h (52). Therefore, despite being unexpected, mtDNA increase, as seen with IPA, can occur even if PGC1α is reduced, reflecting complex mitochondrial regulation.

Regarding PGC1α gene expression, it was significantly different than what was observed in protein content. More specifically, C3G treatment increased PGC1α, gene expression, having C3G a reduced protein content. This shows that transcriptional upregulation was not acutely matched to increased mitochondrial content, either due to dose or timing limitations. As referred before, PGC1α activity itself is transient, peaking a few hours after stimulation (40).

Considering that both mRNA and protein levels were assessed for PGC1α, differences observed for the same treatment likely reflect post-transcriptional regulation, timing, and translation efficiency. This aligns with the view that mitochondrial function is modulated not only at the transcriptional level but also through post-transcriptional mechanisms that adjust protein composition according to cellular metabolic needs and environmental conditions (54).

Mitophagy, as assessed by Parkin protein expression, did not differ significantly between groups. This may indicate that dynamic changes in Parkin recruitment occurred at earlier timepoints and may have plateaued by 24 h (53).

For thermogenesis, UCP1 gene expression was increased in the IR group, suggesting there was heat generated as a result of balancing the proton gradient that was not dissipated through ATP production, due to mitochondrial uncoupling. Conversely, BB and PCA treatments reduce UCP1, indicating improved coupling and energy efficiency, consistent with ATP normalization.

Overall, the use of a cellular model in this study allowed us to shed light on the direct effects of BB and its compounds and metabolites on adipocyte mitochondria, providing mechanistic insights that complement the findings from animal studies.

Proposed Integrative Model of Blackberry, C3G, PCA and IPA Action in Obesity

Based on the present findings, a model integrating these mechanisms can be proposed (Figure 12).

In the context of obesity, IR disrupts mitochondrial coupling, reduces fusion, impairs mitochondria biogenesis, and induces compensatory UCP1 expression as a means to dissipate excess proton gradient. These maladaptive responses are accompanied by elevated ATP and reduced ROS, consistent with a metabolic shift toward glycolytic compensation rather than efficient oxidative phosphorylation.

BB-derived compounds appear to counteract these alterations through complementary, yet distinct, mechanisms. In AT, BB supplementation increased mtDNA content. In 3T3-L1 adipocytes, IPA increased mtDNA levels, consistent with stimulation of biogenesis or preservation of mtDNA integrity. PCA restored mitochondrial dynamics through increasing both MFN2 (fusion) and DRP1 (fission). C3G upregulated PGC1α gene expression but was associated with reduced protein levels and mtDNA content, pointing to a transient or partial activation of the biogenesis pathway. Whole BB extract decreased UCP1 expression and, together with PCA, promoted more efficient OXPHOS, which aligns with the normalization of ATP and ROS levels observed across treatments.

This theoretical and integrative model highlights that no single compound fully restores mitochondrial function. Instead, anthocyanins and their metabolites act through partially overlapping and sometimes divergent pathways whose combined action has an important impact on mitochondrial efficiency. Such complementarity means the effects cannot and should not be attributed to a single compound or metabolite, but to the complex mixture of bioactive compounds present after the consumption of anthocyanin-rich fruits. Notably, the profile and number of

Campo Mártires da Pátria, 130
1169-056 Lisboa · Portugal

metabolites generated will be determined by host metabolism and gut microbiota composition, which is, in turn, dependent on multiple host-related factors. This serves to highlight **why whole-fruit intake may provide benefits that cannot be reproduced by isolated compound supplementation**.

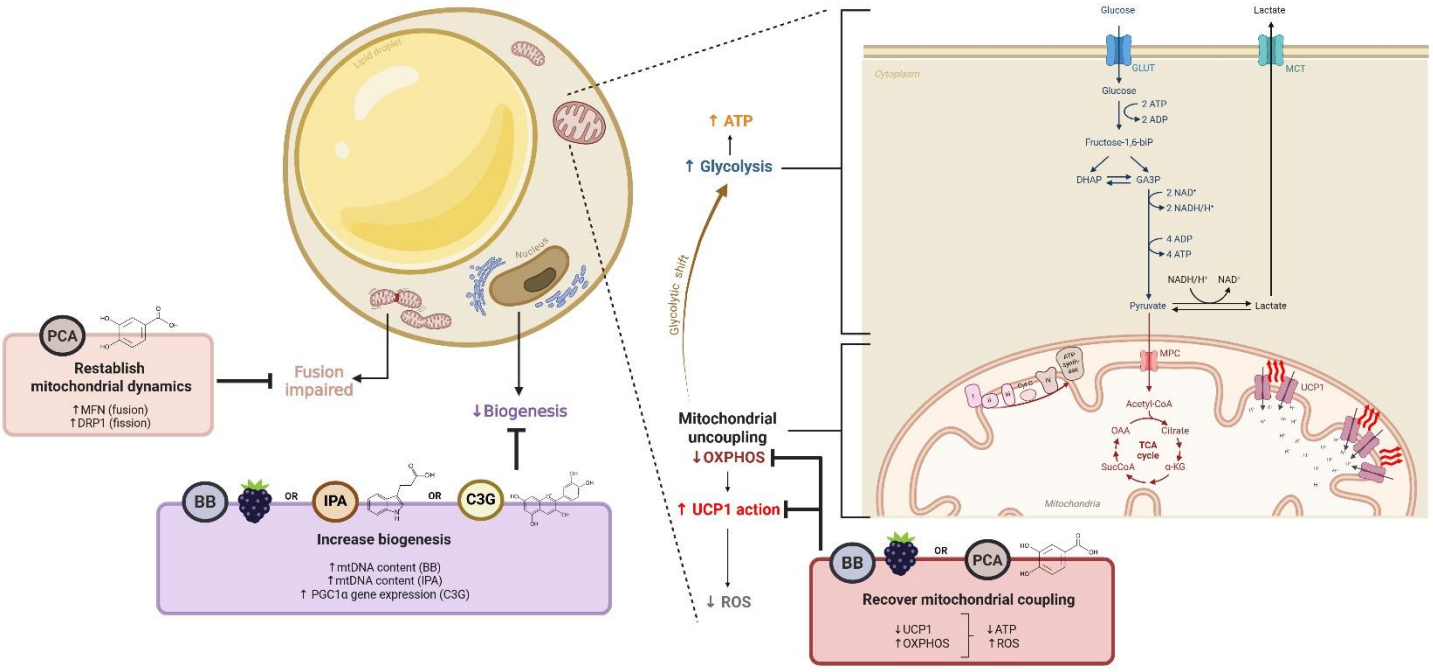

Figure 12. Proposed integrative model of blackberry (BB), cyanidin-3-glucoside (C3G), protocatechuic acid (PCA), and indole-3-propionic acid (IPA) action in obesity. Representation of an insulin resistant adipocyte, characterized by impaired fusion, reduced biogenesis, mitochondrial uncoupling with consequent UCP1 upregulation and heat dissipation, decreased ROS generation, and a glycolytic shift leading to increased glycolysis and ATP production. Treatments counteracted these impairments in specific ways: PCA restored mitochondrial dynamics by increasing MFN2 and DRP1 expression; BB and IPA increased mtDNA content, while C3G upregulated PGC1α gene expression; BB and PCA improved coupling by reducing UCP1 expression and enhancing OXPHOS, leading to lower ATP content and higher ROS generation. Image created with BioRender.com.

Campo Mártires da Pátria, 130
1169-056 Lisboa · Portugal

Conclusion

In conclusion, this work shows that BB can modulate mitochondria dynamics, and that not only the fruit itself but also its compounds and metabolites can modulate mitochondrial function in obesity through compound-specific mechanisms. Using both animal and cellular models, we observed that these compounds act on key mitochondrial processes, including biogenesis, coupling, and thermogenesis, contributing to improved mitochondrial efficiency. While further studies are required to confirm these findings *in vivo* and to establish their translational relevance, our results support the potential of whole anthocyanin-rich berries as promising candidates to counteract mitochondrial dysfunction and metabolic alterations associated with obesity.

Campo Mártires da Pátria, 130
1169-056 Lisboa · Portugal

References

1. World Obesity Federation. *World Obesity Atlas 2025*. London: World Obesity Federation; 2025. Available from: https://s3-eu-west-1.amazonaws.com/wof-files/World_Obesity_Atlas_2025.pdf
2. Guerreiro VA, Carvalho D, Freitas P. Obesity, adipose tissue, and inflammation answered in questions. *J Obes*. 2022 Jan 22;2022:2252516. doi: 10.1155/2022/2252516
3. World Health Organization. Obesity and overweight [Internet]. Geneva: World Health Organization; 2025 May 7 [cited 2025 May 29]. Available from: https://www.who.int/news-room/fact-sheets/detail/obesity-and-overweight
4. The Lancet Diabetes & Endocrinology. Redefining obesity: advancing care for better lives. Lancet Diabetes Endocrinol. 2025 Jan 14;3(1):1-2. doi: 10.1016/S2213-8587(25)00004-X
5. Heymsfield SB, Wadden TA. Mechanisms, pathophysiology, and management of obesity. *N Engl J Med*. 2017 Jan 19;376(3):254-66. doi: 10.1056/NEJMra1514009
6. Khalil M, et al. The potential of the Mediterranean diet to improve mitochondrial function in experimental models of obesity and metabolic syndrome. *Nutrients*. 2022;14(15):3112. doi: 10.3390/nu14153112.
7. Guerrier L, Malpuech-Brugère C, Richard R, Touron J. Mitochondrial Function in Healthy Human White Adipose Tissue: A Narrative Review. *Nutrients*. 2023 Oct 19;15(20):4430. doi: 10.3390/nu15204430.
8. Das S, Mukhuty A, Mullen GP, Rudolph MC. Adipocyte Mitochondria: Deciphering Energetic Functions across Fat Depots in Obesity and Type 2 Diabetes. *Int J Mol Sci*. 2024;25(12):6681. doi: 10.3390/ijms25126681.
9. Todosenko N, Khaziakhmatova O, Malashchenko V, Yurova K, Bograya M, Beletskaya M, Vulf M, Gazatova N, Litvinova L. Mitochondrial Dysfunction Associated with mtDNA in Metabolic Syndrome and Obesity. *Int J Mol Sci*. 2023 Jul 27;24(15):12012. doi: 10.3390/ijms241512012.
10. Xia W, Veeragandham P, Cao Y, Xu Y, Rhyne TE, Qian J, Hung CW, Zhao P, Jones Y, Gao H, Liddle C, Yu RT, Downes M, Evans RM, Rydén M, Wabitsch M, Wang Z, Hakozaki H, Schöneberg J, Reilly SM, Huang J, Saltiel AR, et al. Obesity causes mitochondrial fragmentation and dysfunction in white adipocytes due to RalA activation. *Nat Metab*. 2024 Feb;6(2):273–289. doi: 10.1038/s42255-024-00978-0.
11. Archer SL. Mitochondrial dynamics—mitochondrial fission and fusion in human diseases. *N Engl J Med*. 2013 Dec 5;369(23):2236-51. doi:10.1056/NEJMra1215233.
12. Wang J, Lin X, Zhao N, Dong G, Wu W, Huang K, Fu J. Effects of Mitochondrial Dynamics in the Pathophysiology of Obesity. *Front Biosci (Landmark Ed)*. 2022 Mar 18;27(3):107. doi: 10.31083/j.fbl2703107
13. Alappat B, Alappat J. Anthocyanin Pigments: Beyond Aesthetics. *Molecules*. 2020;25(22):5500. doi:10.3390/molecules25235500.
14. Song W, Yuan Q, Wang Y, Mai M, Luo M, Guo H. Anthocyanin supplementation improves obesity-related inflammatory characteristics: A systematic review and meta-analysis of randomized controlled trials. *Nutr Res*. 2023;116:1-11. doi:10.1016/j.nutres.2023.05.009.
15. Ngamsamer C, Sirivarasai J, Sutjarit N. The benefits of anthocyanins against obesity-induced inflammation. *Biomolecules*. 2022;12:852. doi:10.3390/biom12060852.
16. Oumeddour DZ, Al-Dalali S, Zhao L, Zhao L, Wang C. Recent advances on cyanidin-3-O-glucoside in preventing obesity-related metabolic disorders: A comprehensive review. *Biochem Biophys Res Commun*. 2024;729:150344. doi:10.1016/j.bbrc.2024.150344.
17. Bhosale SS, Granato D, Mohammadi N. Purification and characterization of anthocyanin from Irish wild blackberry: impact on color, composition, and antioxidant capacity. *J Food Meas Charact*. 2025;19(4):2730–2738. doi:10.1007/s11694-025-03142-8.

Campo Mártires da Pátria, 130
1169-056 Lisboa · Portugal

18. Olivas-Aguirre FJ, Rodrigo-García J, del R Martínez-Ruiz N, Cárdenas-Robles AI, Mendoza-Díaz SO, Álvarez-Parrilla E, González-Aguilar GA, de la Rosa LA, Ramos-Jiménez A, Wall-Medrano A. Cyanidin-3-O-glucoside: Physical-Chemistry, Foodomics and Health Effects. *Molecules*. 2016 Sep 21;21(9):1264. doi: 10.3390/molecules21091264.
19. Tan J, Li Y, Hou D-X, Wu S. The effects and mechanisms of cyanidin-3-glucoside and its phenolic metabolites in maintaining intestinal integrity. *Antioxidants (Basel)*. 2019;8(10):479. doi:10.3390/antiox8100479.
20. Tang Z. Cyanidin-3-glucoside: targeting atherosclerosis through gut microbiota and anti-inflammation. *Front Nutr*. 2025 Jun 30;12:1627868. doi: 10.3389/fnut.2025.1627868.
21. Marques C, Fernandes I, Meireles M, Faria A, Spencer JPE, Mateus N, Calhau C. Gut microbiota modulation accounts for the neuroprotective properties of anthocyanins. *Sci Rep*. 2018;8(1):11341. doi:10.1038/s41598-018-29744-5.
22. Fornasaro S, Ziberna L, Gasperotti M, Tramer F, Vrhovšek U, Mattivi F, Passamonti S. Determination of cyanidin 3-glucoside in rat brain, liver and kidneys by UPLC/MS-MS and its application to a short-term pharmacokinetic study. *Sci Rep*. 2016 Mar 11;6:22815. doi:10.1038/srep22815.
23. Solverson P, Albaugh GP, Debelo HA, Ferruzzi MG, Baer DJ, Novotny JA. Mixed Berry Juice and Cellulose Fiber Have Differential Effects on Peripheral Blood Mononuclear Cell Respiration in Overweight Adults. *Nutrients*. 2023;15(7):1709. doi:10.3390/nu15071709.
24. Du L, Ding X, Zhang W, et al. Anthocyanins from blueberry and blackberry ameliorate metabolic syndrome by Prevotella histicola and acetic acid. *npj Sci Food*. 2025;9:158. doi:10.1038/s41538-025-00526-4.
25. Solverson P, Albaugh GP, Harrison DJ, Luthria DL, Baer DJ, Novotny J. High-dose administration of purified cyanidin-3-glucose or a blackberry extract causes improved mitochondrial function but reduced content in 3T3-L1 adipocytes. *Front Nutr*. 2022; (1–9). doi:10.1002/fft2.139.
26. Marino F, Petrella L, Cimmino F, Pizzella A, Monda A, Allocca S, Rotondo R, D'Angelo M, Musco N, Iommelli P, Catapano A, Bagnato C, Paolini B, Cavaliere G. From Obesity to Mitochondrial Dysfunction in Peripheral Tissues and in the Central Nervous System. *Biomolecules*. 2025;15(5):638. doi:10.3390/biom15050638.
27. Flori L, Galgani G, Bray G, Ippolito C, Segnani C, Pellegrini C, Citi V, Bernardini N, Martelli A, Calderone V. Development of an adipocyte differentiation protocol using 3T3-L1 cells for the investigation of the browning process: identification of the PPAR-γ agonist rosiglitazone as a browning reference drug. *Front Pharmacol*. 2025;16:1546456. doi:10.3389/fphar.2025.1546456.
28. Takanezawa Y, Nakamura R, Ohshiro Y, Uraguchi S, Kiyono M. Gadolinium-based contrast agents suppress adipocyte differentiation in 3T3-L1 cells. *Toxicol Lett*. 2023;383:196–203. doi:10.1016/j.toxlet.2023.07.003.
29. Chang E, Choi JM, Park SE, Rhee EJ, Lee WY, Oh KW, Park SW, Park CY. Adiponectin deletion impairs insulin signaling in insulin-sensitive but not insulin-resistant 3T3-L1 adipocytes. *Life Sciences*. 2015;132:93–100. doi:10.1016/j.lfs.2015.02.013.
30. Kim H, Xue X. Detection of total reactive oxygen species in adherent cells by 2',7'-dichlorodihydrofluorescein diacetate staining. *J Vis Exp*. 2020;(160):60682. doi:10.3791/60682.
31. Quiros PM, Goyal A, Jha P, Auwerx J. Analysis of mtDNA/nDNA ratio in mice. *Curr Protoc Mouse Biol*. 2017 Mar 2;7(1):47–54. doi:10.1002/cpmo.21.
32. Guo W, Jiang L, Bhasin S, Khan SM, Swerdlow RH. DNA extraction procedures meaningfully influence qPCR-based mtDNA copy number determination. *Mitochondrion*. 2009 Jul;9(4):261–5. doi:10.1016/j.mito.2009.03.003.
33. Lee JH, Park A, Oh K-J, Lee SC, Kim WK, Bae K-H. The role of adipose tissue mitochondria: regulation of mitochondrial function for the treatment of metabolic diseases. *Int J Mol Sci*. 2019 Oct 4;20(19):4924. doi:10.3390/ijms20194924.

Campo Mártires da Pátria, 130
1169-056 Lisboa · Portugal

34. Masschelin PM, Cox AR, Chernis N, Hartig SM. The impact of oxidative stress on adipose tissue energy balance. *Front Physiol*. 2020 Jan 22;10:1638. doi: 10.3389/fphys.2019.01638.
35. Zheng Y, Yang N, Pang Y, Gong Y, Yang H, Ding W, et al. Mitochondria-associated regulation in adipose tissues and potential reagents for obesity intervention. *Front Endocrinol (Lausanne)*. 2023 Jun 16;14:1132342. doi:10.3389/fendo.2023.1132342.
36. Vendrame S, Klimis-Zacas D. Potential factors influencing the effects of anthocyanins on blood pressure regulation in humans: a review. *Nutrients*. 2019 Jun 25;11(6):1431. doi:10.3390/nu11061431.
37. Cassidy A, Minihane AM. The role of metabolism (and the microbiome) in defining the clinical efficacy of dietary flavonoids. *Am J Clin Nutr*. 2017 Jan;105(1):10-22. doi:10.3945/ajcn.116.136051.
38. Azzini E, Giacometti J, Russo GL. Antiobesity effects of anthocyanins in preclinical and clinical studies. *Oxid Med Cell Longev*. 2017;2017:2740364. doi:10.1155/2017/2740364.
39. Jiang H, Zhang W, Li X, Xu Y, Cao J, Jiang W. The anti-obesogenic effects of dietary berry fruits: a review. *Food Res Int*. 2021;147:110539. doi:10.1016/j.foodres.2021.110539.
40. Pilegaard H, Saltin B, Neufer PD. Exercise induces transient transcriptional activation of the PGC-1α gene in human skeletal muscle. *J Physiol*. 2003 Jan 3;546(Pt 3):851-8. doi:10.1113/jphysiol.2002.034850.
41. Shapira SN, Seale P. Transcriptional control of brown and beige fat development and function. *Obesity (Silver Spring)*. 2019 Jan;27(1):13-21. doi:10.1002/oby.22334.
42. Saito M, Matsushita M, Yoneshiro T, Okamatsu-Ogura Y. Brown adipose tissue, diet-induced thermogenesis, and thermogenic food ingredients: from mice to men. *Front Endocrinol (Lausanne)*. 2020 Apr 21;11:222. doi:10.3389/fendo.2020.00222.
43. Matthias A, Ohlson KB, Fredriksson JM, Jacobsson A, Nedergaard J, Cannon B. Thermogenic responses in brown fat cells are fully UCP1-dependent. UCP2 or UCP3 do not substitute for UCP1 in adrenergically or fatty acid-induced thermogenesis. *Journal of Biological Chemistry*. 2000 Aug 18;275(33):25073-81. doi:10.1074/jbc.M000547200.
44. Ceddia RP, Liu D, Shi F, Crowder MK, Mishra S, Kass DA, et al. Increased energy expenditure and protection from diet-induced obesity in mice lacking the cGMP-specific phosphodiesterase PDE9. *Diabetes*. 2021 Dec;70(12):2823-36. doi:10.2337/db21-0100.
45. Cremonini E, Da Silva LME, Lanzi CR, Marino M, Iglesias DE, Oteiza PI. Anthocyanins and their metabolites promote white adipose tissue beiging by regulating mitochondria thermogenesis and dynamics. *Biochem Pharmacol*. 2024 May;222:116069. doi: 10.1016/j.bcp.2024.116069.
46. Gomes JVP, Rigolon TCB, da Silveira Souza MS, Alvarez-Leite JI, Della Lucia CM, Stampini Duarte Martino H, Rosa COB. Antiobesity effects of anthocyanins on mitochondrial biogenesis, inflammation, and oxidative stress: A systematic review. *Nutrition*. 2019 Oct;66:192-202. doi:10.1016/j.nut.2019.05.005.
47. Alberts B, Johnson A, Lewis J, Morgan D, Raff M, Roberts K, Walter P. Molecular biology of the cell. 6th ed. New York: Garland Science; 2015.
48. Yang C, Aye CC, Li X, Diaz Ramos A, Zorzano A, Mora S. Mitochondrial dysfunction in insulin resistance: differential contributions of chronic insulin and saturated fatty acid exposure in muscle cells. *Biosci Rep*. 2012 Oct;32(5):465–78. doi:10.1042/BSR20120034.
49. Zeng Y, Guo M, Wu Q, Tan X, Jiang C, Teng F, et al. Gut microbiota-derived indole-3-propionic acid alleviates diabetic kidney disease through its mitochondrial protective effect via reducing ubiquitination mediated-degradation of SIRT1. *J Adv Res*. 2025 Jul;73:607-30. doi:10.1016/j.jare.2024.08.018.
50. Adebayo M, Singh S, Singh AP, Dasgupta S. Mitochondrial fusion and fission: The fine-tune balance for cellular homeostasis. *FASEB J*. 2021 Jun;35(6):e21620. doi: 10.1096/fj.202100067R.
51. Chen W, Zhao H, Li Y. Mitochondrial dynamics in health and disease: mechanisms and potential targets. *Signal Transduct Target Ther*. 2023;8:333. doi:10.1038/s41392-023-01547-9.
52. Cantó C, Auwerx J. PGC-1α, SIRT1 and AMPK, an energy sensing network that controls energy expenditure. *Curr Opin Lipidol*. 2009;20(2):98–105. doi:10.1097/MOL.0b013e328328d0a4.

Campo Mártires da Pátria, 130
1169-056 Lisboa · Portugal

53. Narendra D, Tanaka A, Suen DF, Youle RJ. Parkin is recruited selectively to impaired mitochondria and promotes their autophagy. *J Cell Biol. 2008 Nov* 24;183(5):795-803. doi:10.1083/jcb.200809125.

54. Tsuboi T, Leff J, Zid BM. Post-transcriptional control of mitochondrial protein composition in changing environmental conditions. *Biochem Soc Trans*. 2020;48(6):2565–78. doi:10.1042/BST20200250.

Campo Mártires da Pátria, 130
1169-056 Lisboa · Portugal

Supplemental Materials

Appendix 1 - Approval by DGAV

REPÚBLICA PORTUGUESA
AGRICULTURA E ALIMENTAÇÃO

dgav

Exma. Sra.
Dra. Cláudia Fernandes
Nova Medical School, Universidade Nova de Lisboa
Campo Mártires da Pátria, 130
1169-056 Lisboa

2023-05-24 008695

Nossa referência	Vossa referência	Vossa data
0421/000/000/2023		

Assunto: PROTEÇÃO DOS ANIMAIS UTILIZADOS PARA FINS CIENTÍFICOS E/OU OUTROS FINS CIENTÍFICOS – PEDIDO DE AUTORIZAÇÃO PARA REALIZAÇÃO DE PROJETO DE EXPERIMENTAÇÃO ANIMAL

Na sequência do pedido efetuado por V. Exª no sentido de poder ser autorizada a realização do projeto experimental designado "*MONET- O desafio do eixo microbiota-intestino-cérebro na neuroinflamação associada à obesidade: o papel do consumo de amora*", tendo como investigadora responsável a Doutora Ana Isabel Gonçalves Faria, cabe-me informar que o mesmo foi avaliado de acordo com o Artigo 44º do Decreto-Lei n.º 113/2013, de 7 de agosto, relativo à "proteção dos animais utilizados para fins científicos". Sendo o resultado desta avaliação favorável, informa-se V. EX.ª que o projeto em apreço foi autorizado de acordo com o n.º 1, do Artigo 42º do mesmo diploma legislativo.

Reforça-se ainda, que deverá existir uma apertada monitorização dos sinais de dor, sofrimento ou angústia dos animais submetidos aos procedimentos, para que a aplicação dos limites críticos estabelecidos para cada um dos procedimentos se faça de forma adequada a cada animal, tendo em conta a necessidade de impedir que os sinais de dor, sofrimento ou angústia severos se prolonguem sem a tomada de medidas mitigantes dos mesmos. A monitorização dos sinais de dor, sofrimento ou angústia dos animais

Campo Grande, n.º 50 | 1700-093 Lisboa
Tlf.: 213 239 500

1/3

REPÚBLICA PORTUGUESA
AGRICULTURA E ALIMENTAÇÃO

dgav

submetidos aos procedimentos, classificados prospectivamente em termos de severidade nas categorias ligeira, moderada e severa, deverá ser feita no sentido de se atualizar a severidade efetiva a que os mesmos ficarão, na realidade, sujeitos.

Finalmente, resta-me especificar, de acordo, com o discriminado no n.º 2, do Artigo 46º, do atrás referido Decreto-Lei, o seguinte:

- **O utilizador que realiza o projeto:** Senhor Reitor da Universidade Nova de Lisboa, Professor Doutor João Sàágua;
- **A pessoa responsável pela execução global do projeto e pela sua conformidade com a autorização do mesmo:** Doutora Ana Faria
- **O estabelecimento onde o projeto vai ser realizado:** Biotério da Faculdade de Medicina da Universidade Nova de Lisboa

Com os melhores cumprimentos,

A Diretora de Serviços de Proteção Animal

Ana Cláudia Nunes
Chefe de Divisão
de Epidemiologia e
Saúde Animal

Anexo: Requerimento de autorização de projeto

DSPA-DBEA/ SBX
Campo Grande, n.º 50 | 1700-093 Lisboa
Tlf.: 213 239 500

Campo Mártires da Pátria, 130
1169-056 Lisboa · Portugal

Appendix 2 - Approval by ORBEA of NMS | UNL

NOVA MEDICAL SCHOOL

PARECER

Título do projeto: **"MONET- O desafio do eixo microbiota-intestino-cérebro na neuroinflamação associada à obesidade: o papel do consumo de amora"**

Referência do projeto: **22_01_ORBEA**

Investigador Responsável: **Professora Doutora Ana Isabel Gonçalves Faria**

Instituição: Faculdade de Ciências Médicas | NOVA Medical School da Universidade NOVA de Lisboa

O Órgão Responsável pelo Bem-Estar dos Animais (ORBEA) da Faculdade de Ciências Médicas | NOVA Medical School da Universidade NOVA de Lisboa procedeu a uma cuidada avaliação do projeto acima indicado de acordo com os requisitos da legislação portuguesa que se aplica à utilização de animais para fins científicos. Considera-se que estão descritos adequadamente os métodos e procedimentos propostos e que está assegurado o bem-estar dos animais a utilizar. O responsável pela utilização de animais deste projeto é detentor de uma licença individual, bem como todos os intervenientes no contacto com animais.

Assim, o parecer do ORBEA da Faculdade de Ciências Médicas | NOVA Medical School da Universidade NOVA de Lisboa é favorável à realização do projeto em epígrafe. Qualquer alteração futura aos procedimentos descritos que possam interferir com o bem-estar animal, número de animais ou os elementos da equipa, exige uma reapresentação de pedido de apreciação a este Orgão.

Lisboa, 20 de dezembro de 2022

AJSantos

Prof.ª Doutora Ana Isabel Moura Santos
(Presidente do ORBEA)

Campo Mártires da Pátria, 130
1169-056 Lisboa · Portugal

Campo Mártires da Pátria, 130
1169-056 Lisboa · Portugal

www.nms.unl.pt

Appendix 3 - Approval by the Ethical Committee of NMS | UNL

Decisão final sobre o projeto

"MONET- O desafio do eixo microbiota-intestino-cérebro na neuroinflamação associada à obesidade: o papel do consumo de amora"

A Comissão de Ética da NMS|FCM-UNL (CEFCM) decidiu, aprovar por unanimidade, do ponto de vista ético, o projeto de investigação intitulado "***MONET- O desafio do eixo microbiota-intestino-cérebro na neuroinflamação associada à obesidade: o papel do consumo de amora"*** (nº 114/2021/CEFCM), submetido pela Investigadora Principal, Profa. Doutora Ana Isabel Gonçalves Faria.

Lisboa, 25 de novembro de 2021

O Presidente da Comissão de Ética,

(Professor Doutor Diogo Pais)

TO WHOM IT MAY CONCERN

The Ethics Research Committee of NMS|FCM-UNL (CEFCM) has unanimously approved, the Project entitled "***MONET- O desafio do eixo microbiota-intestino-cérebro na neuroinflamação associada à obesidade: o papel do consumo de amora"*** (No. 114/2021/CEFCM) submitted by the Principal Investigator, Ana Isabel Gonçalves Faria, PhD.

Lisbon, November 25th, 2021

The Chairman of the Ethics Research Committee,

(Diogo Pais, MD, PhD)

Campo Mártires da Pátria, 130
1169-056 Lisboa · Portugal

www.nms.unl.pt

Appendix 4 - Expression of target genes related to mitochondrial function in differentiated 3T3-L1 adipocytes

Table S1. Expression of target genes related to mitochondrial function in differentiated 3T3-L1 adipocytes, comparing control (Ø) and IR groups.

	Ø	IR	*p* value
	(*n* = 4)	(*n* = 4)	
mPPARγ	0.00509 (1.5x10^{-3})	0.00676 (2.3x10^{-3})	0.2723
mMCP1	12.28 (1.4)	11.18 (0.7)	0.2629
AhR	0.00072 (1.7x10^{-4})	0.00045 (2.0x10^{-4})	0.1548

Table S2. Expression of target genes related to mitochondrial function in differentiated 3T3-L1 adipocytes, comparing control (Ø) and BB groups.

	Ø	BB	*p* value
	(*n* = 4)	(*n* = 4)	
mPPARγ	0.00509 (1.5x10^{-3})	0.00546 (1.9x10^{-3})	0.7672
mMCP1	12.28 (1.4)	12.76 (3.1)	0.7862
AhR	0.00072 (1.7x10^{-4})	0.00385 (2.1x10^{-3})	0.0631

Table S3. Expression of target genes related to mitochondrial function in differentiated 3T3-L1 adipocytes, comparing control (Ø) and Cy3g groups.

	Ø	Cy3g	*p* value
	(*n* = 4)	(*n* = 4)	
mPPARγ	0.00509 (1.5x10^{-3})	0.00670 (1.9x10^{-3})	0.2645
mMCP1	12.28 (1.4)	10.79 (1.5)	0.1918
AhR	0.00072 (1.7x10^{-4})	0.00117 (1.8x10^{-4})	0.0696

Table S4. Expression of target genes related to mitochondrial function in differentiated 3T3-L1 adipocytes, comparing control (Ø) and IPA groups.

	Ø	IPA	*p* value
	(*n* = 4)	(*n* = 4)	
mPPARγ	0.00509 (1.5x10^{-3})	0.00456 (1.3x10^{-3})	0.6090
mMCP1	12.28 (1.4)	11.33 (1.6)	0.3923
AhR	0.00072 (1.7x10^{-4})	0.00554 (5.7x10^{-3})	0.2110

Table S5. Expression of target genes related to mitochondrial function in differentiated 3T3-L1 adipocytes, comparing control (Ø) and PCA groups.

	Ø	PCA	*p* value
	(*n* = 4)	(*n* = 4)	
mPPARγ	0.00509 (1.5x10^{-3})	0.00582 (1.6x10^{-3})	0.5261
mMCP1	12.28 (1.4)	10.93 (1.5)	0.2269
AhR	0.00072 (1.7x10^{-4})	0.00052 (2.4x10^{-4})	0.3049

Campo Mártires da Pátria, 130
1169-056 Lisboa · Portugal

NOVA MEDICAL SCHOOL

UNIVERSIDADE NOVA DE LISBOA

nms.unl.pt